

Kansas City PM Characterization Study

Final Report

Appendix MM

Gas Diesel Split Study

Assessment and Standards Division
Office of Transportation and Air Quality
U.S. Environmental Protection Agency

Sponsors:

National Renewable Energy Laboratory, U.S. Department of Energy
Federal Highway Administration, U.S. Department of Transportation
STAPPA-ALAPCO Emission Inventory Improvement Program
Coordinating Research Council Inc. (Project No. E-69)

Prepared for EPA by
Eastern Research Group, Incorporated
Austin, TX

Bevilacqua-Knight Incorporated
Oakland, CA

NuStats LLC
Austin, TX

Desert Research Institute
Reno, NV

EPA Contract No. GS 10F-0036K

October 27, 2006
Revised April 2008 by EPA staff



United States
Environmental Protection
Agency

EPA420-R-08-009
April 2008

**Variations in Speciated Emissions from Spark-Ignition and Compression-Ignition
Motor Vehicles in California's South Coast Air Basin**

Eric M. Fujita*, Barbara Zielinska, David E. Campbell, W. Patrick Arnott, John C. Sagebiel,
Lynn Rinehart ^a and Judith C. Chow
Desert Research Institute Division of Atmospheric Sciences

Peter A. Gabele ^b, William Crews ^c and Richard Snow ^c
Source Apportionment and Characterization Branch, MD-46
National Exposure Research Laboratory
^c Bevilacqua-Knight, Inc., MD-8
U.S. Environmental Protection Agency
Research Triangle Park, NC 27711

Nigel N. Clark and W. Scott Wayne
Department of Mechanical and Aerospace Engineering
West Virginia University
123/125 Engineering Sciences Building
P.O. Box 6106
Morgantown, WV 26506

Douglas R. Lawson
National Renewable Energy Laboratory
1617 Cole Blvd.
Golden, CO 80401

* Corresponding author, phone: (775) 674-7084; fax: (775) 674-7060; e-mail:
Eric.Fujita@dri.edu.

^a Colorado State University, Fort Collins, CO

^b Retired

ABSTRACT

The DOE Gasoline/Diesel PM Split Study examined the sources of uncertainties in using an organic compound-based chemical mass balance (CMB) receptor model to quantify the contributions of spark-ignition (SI) and compression-ignition (CI) engine exhaust to ambient fine particulate matter (PM_{2.5}). This paper presents the chemical composition profiles of SI and CI engine exhaust from the vehicle testing portion of the study. Chemical analysis of source samples consisted of gravimetric mass, elements, ions, organic and elemental carbon (OC and EC) by both the IMPROVE and STN thermal/optical methods, polycyclic aromatic hydrocarbons, hopanes, steranes, alkanes, and polar organic compounds. Over half the mass of

carbonaceous particles emitted by heavy-duty diesel trucks was EC (IMPROVE) and emissions from SI vehicles contained predominantly OC. While total carbon (TC) by the IMPROVE and STN protocols agreed well for all samples, the STN/IMPROVE ratios for EC from SI exhaust decreased with decreasing sample loading. SI vehicles, whether low or high emitters, emitted greater amounts of high molecular-weight particulate PAHs (benzo(ghi)perylene, indeno(1,2,3-cd)pyrene, and coronene) than CI vehicles. Diesel emissions contained higher abundances of 2- to 4-ring semi-volatile PAHs. Diacids were emitted by CI vehicles, but are also prevalent in secondary organic aerosols so they cannot be considered unique tracers. Hopanes and steranes were present in lubricating oil with similar composition for both gasoline and diesel vehicles and were negligible in gasoline or diesel fuels. CI vehicles emitted greater total amounts of hopanes and steranes on a mass per mile basis, but abundances were comparable to SI exhaust normalized to TC emissions within measurement uncertainty. The combustion-produced high-molecular weight PAHs were found in used gasoline motor oil but not in fresh oil and are negligible in used diesel engine oil. The contributions of lubrication oils to abundances of these PAHs in the exhaust were large in some cases and were variable with the age and consumption rate of the oil. These factors contributed to the observed variations in their abundances to total carbon or $PM_{2.5}$ among the SI composition profiles.

IMPLICATIONS

We examined several factors that contribute to variations in chemical composition of $PM_{2.5}$ emissions from in-use diesel and gasoline vehicles in California's South Coast Air Basin. These factors included model year, mileage accumulation, vehicle test cycles, composition of lubrication oils and variations in sampling and analytical methods. Distinctive differences were found in the abundances of specific chemical species in diesel and gasoline exhaust, but the variations among individual exhaust profiles were large. These variations should be considered when applying specific profiles in receptor modeling or emission inventory development and in estimating the uncertainties associated with the results.

ABOUT THE AUTHORS

Eric Fujita and Barbara Zielinska are Research Professors, David Campbell is an Assistant Research Scientist, John C. Sagebiel is an Assistant Research Professor, and Judith Chow is a

Research Professor in the Division of Atmospheric Sciences at the Desert Research Institute (Nevada System of Higher Education). William “Pat” Arnott is an Associate Professor in the Department of Physics at the University of Nevada, Reno. Lynn Rinehart is a post-doctoral fellow in the Atmospheric Science Department/Cooperative Institute for Research in the Atmosphere at Colorado State University. Douglas R. Lawson is a Principle Scientist at the National Renewable Energy Laboratory. Nigel N. Clark is a Professor and W. Scott Wayne is a Research Assistant Professor of Mechanical and Aerospace Engineering at West Virginia University. Peter A. Gabele is retired from the U.S. Environmental Protection Agency. William Crews and Richard Snow are with Bevilacqua Knight, Inc. Address correspondence to: Eric M. Fujita, Division of Atmospheric Sciences at the Desert Research Institute, 2215 Raggio Parkway, Reno, NV, 89512; phone: (775) 674-7084; fax: (775) 674-7060; e-mail: Eric.Fujita@dri.edu.

INTRODUCTION

Motor vehicle emissions are important sources of ambient air pollution and have been statistically associated with cancer and non-cancer health effects.¹⁻² Vehicle exhaust is a complex mixtures of particulate matter (PM), gaseous pollutants and semi-volatile organic compounds (SVOC) that are in equilibrium with the particle phase. Several studies have been conducted recently to characterize the emission rates and organic speciation of PM from gasoline (or spark-ignition, SI) and diesel (or compression-ignition CI) vehicles.³⁻¹² The rate and chemical composition of gaseous and particulate emissions from diesel and gasoline vehicles depend upon many factors, which include vehicle age and mileage, fuel, emission control technology, state of vehicle maintenance, type and condition of lubricating oil, vehicle operating mode (e.g., cold start, hot stabilized), engine load, and ambient temperature. Data from dynamometer exhaust emission tests of properly functioning light-duty gasoline vehicles show that modern, low-mileage vehicles have low carbon monoxide, hydrocarbon, and particulate matter emission rates during hot stabilized operation and during relatively non-aggressive driving conditions.^{13,14} Emission rates are higher for properly functioning vehicles during cold starts, during intermittent high engine load conditions induced by hard acceleration and grade and at low ambient temperatures.^{10,13,14} The distribution of emission rates among in-use vehicles is highly skewed with a relatively small fraction of high emitters accounting for a disproportionate fraction of total emissions.^{4,15,16}

Receptor models have been widely used to estimate the contributions of various sources to measured airborne particulate matter concentrations.^{3, 5} Current understanding of the uncertainties associated with receptor modeling calculations is limited by data to sufficiently characterize the variations and representativeness of source composition profiles, especially for motor vehicles. The Gasoline/Diesel PM Split Study was conducted during the summer of 2001 to assess the sources of uncertainties in using organic-compound-based chemical mass balance (BMV) receptor model to quantify the relative contributions of emissions from SI and CI engines to the ambient concentrations of fine particulate matter (PM_{2.5}). The impetus for the study was the disparate conclusions obtained from studies in the Los Angeles area and the Northern Front Range of Colorado regarding the relative contributions of SI and CI vehicles to ambient concentrations of fine particles.^{3,5,6} Studies conducted in Denver indicated that gasoline combustion from mobile sources contributed more to ambient PM than diesel combustion. However, studies conducted in Los Angeles indicate that diesel combustion contributed more than gasoline combustion to ambient PM.

Key components of the design for the Gasoline/Diesel PM Split Study included characterization of the variations in exhaust composition within vehicle categories, the differences in determination of elemental carbon by two alternative methods, and comparability between multiple laboratories in the analysis of organic species. The study called for researchers from the Desert Research Institute (DRI) and the University of Wisconsin Madison (UWM) to work cooperatively on sample collection and quality assurance aspects of the study, but work independently, at least initially, on chemical analysis and data analysis. This current study did not necessarily seek to reconcile the results of the prior studies, but was intended to examine the range of uncertainties that may be associated with the methods and procedures for sample collection, chemical analysis, and source apportionment. This paper presents the source composition profiles derived by the DRI. It examines variations in the relative abundances of OC, EC, and potential molecular markers in SI and CI exhaust relative to the factors that may be associated with the observed variations. The ambient source apportionment results obtained by DRI and associated uncertainties are described elsewhere.^{17,18}

EXPERIMENTAL METHODS

As part of this collaborative study, Bevilacqua-Knight, Inc. (BKI) with the U.S. Environmental Protection Agency (EPA) and West Virginia University (WVU) conducted dynamometer tests of light-duty gasoline-powered vehicles and heavy-duty diesel-powered vehicles, respectively. The vehicle emission tests were conducted at the Ralphs Grocery distribution center in Riverside, CA during summer of 2001 from June 2 to June 23 for light-duty vehicles, and from July 20 to September 19 for heavy-duty diesel vehicles. The vehicle selection and test protocols, vehicle characteristics, and dynamometer systems are described by EPA and BKI and WVU.^{19,20} Details of the testing program that are pertinent to the development of exhaust composition profiles are summarized here.

Light-Duty Vehicle Testing

The U.S. Environmental Protection Agency (EPA) and BKI conducted dynamometer tests on their transportable Clayton Model CTE-50-0 chassis dynamometer for 57 light-duty gasoline vehicles and two light-duty diesel vehicles in the eleven combined model-year and mileage categories shown in Table 1. Table S1, located in the supplemental information section, gives the make, model, model year, mileage, and PM_{2.5} emission rates for each vehicle.

Regulated emissions were determined with a constant volume sampling system (CVS) and continuous monitors for carbon monoxide (CO), carbon dioxide (CO₂), total hydrocarbons (THC), and oxides of nitrogen (NO_x). BKI tested each vehicle using a modified Unified Driving Cycle (UDC) that consisted of a phase 1 plus phase 2 from a cold start, a ten minute soak, followed immediately by a repeat of the phase 1 (i.e., phase 3) plus phase 2 from a warm start. A pair of time-integrated samples was collected for each vehicle, one during phases 1 and 2 of the test cycle ("cold start" sample) and a second during the repeat of phases 1 and 2 after the ten-minute soak ("warm start" sample). The warm start test was repeated for eight vehicles to investigate the reproducibility of the emissions. In two of the replicate tests a set of parallel samples was collected from a smaller residence chamber with a volume equal to 20 percent of the main chamber (60 liters) to investigate the extent of particle coagulation and condensation.

One composite sample was collected for each model year and mileage group in categories 1 through 4 by sampling all vehicles within each category through the same sampling media (“media composite”). Samples were collected on separate media for vehicles in all remaining vehicle categories and combined in the laboratory according to the scheme shown in Table S1. Selection of samples within the composites were based on a target minimum combined mass loading of 1 mg of OC, which was estimated by subtracting the photoacoustic black carbon (BC) from gravimetric mass. The analytical composites also combined samples with similar BC/PM_{2.5} ratios. Other relevant chemical characterizations included lubricating oils from each vehicle and representative fuel samples from nearby service stations. The lubrication oil samples were analyzed by DRI for organic constituents and by Gregory Poole Laboratories in Raleigh, NC for elements by inductively coupled plasma (ICP) analysis.

Heavy-Duty Diesel Vehicle Testing

West Virginia University (WVU) tested heavy-duty diesel trucks and diesel buses on their transportable heavy-duty vehicle emissions testing laboratories. Thirty trucks were selected for testing in the twelve combined vehicle weight (light-heavy, medium-heavy and heavy-heavy) and model year categories shown in Table 2. Fifteen trucks were newer model year, well-maintained fleet vehicles. The remaining fifteen trucks were a mix of vehicles in typical service. Two transit buses were also tested with one transit bus representing older engine technology and one representing newer engine technology. All 30 trucks were operated over three duty cycles for purposes of developing composition profiles, the City-Suburban Heavy Vehicle Route (CSHVR), the highway cycle (HW), and idle operation. The two buses were operated through the CSHVR, an idle period, and the Manhattan test cycle. WVU recorded continuous emissions levels of NO_x, THC, CO, and CO₂. PM mass emissions were measured using two parallel filter-sampling trains. PM emissions were also continuously measured by WVU using a Tapered Element Oscillating Microbalance. An oil sample was withdrawn from each engine tested, and analyzed by DRI for organic constituents.

A set of time-integrated samples was collected in parallel by DRI and UWM for each test cycle run on each vehicle. When possible, the secondary dilution ratio was adjusted to compensate for variations in the emission rate of the vehicles. Table S2, in the supplemental

information section, gives the make, model, model year, mileage, and PM_{2.5} emission rates for each vehicle, and shows which samples were combined into composite samples. Analytical results for the idle tests are not shown because mass loadings were too low to yield useable data.

Sample Collection and Continuous Measurements

DRI provided a secondary dilution sampler that was capable of collecting diluted exhaust samples from the primary dilution tunnels of the EPA and WVU transportable dynamometers. The DRI dilution sampler was tested by Chang et al.²¹ and is based on a similar sampler originally designed by Hildemann et al.²² Emissions were withdrawn from the primary exhaust dilution tunnel through a heated Teflon line to the dilution sampler. In the sampler the exhaust mixed with dilution air under turbulent flow conditions, to cool and dilute the exhaust to near-ambient conditions. Ambient air filtered through a high efficiency particulate air (HEPA) filter and an activated carbon bed was used for dilution. The secondary dilution was adjusted to ratios between 20 and 50 for diesel testing. Several diesel trucks were also retested without secondary dilution as part of another project. Due to the large range of emission rates for different test cycles and vehicles, the optimal sampling rate could not always be achieved for all sampling media. For example, sample loading was excessive in some samples for TOR carbon analysis but was optimal for organic speciation. In general, the range of PM emissions for diesel trucks were lower than expected resulting in many diluted exhaust samples with near or below detection quantities for most organic species. For SI vehicles, the secondary dilution sampler was used without dilution (i.e., as a residence time chamber only) due to the low PM emission rates expected for most SI vehicles.

Sample air from the secondary dilution sampler was distributed to the various samplers from a conical aluminum plenum with 12 exit ports distributed radially around its base. From the residence chamber the samples were drawn through cyclone separators with a cut-off diameter of 2.5 µm, operating at 113 lpm, and collected using a DRI sequential filter sampler for inorganic species, and the DRI sequential fine particulate/semi-volatile organic compound (PSVOC) sampler for organic species (10). Samples were also collected by UWM in parallel with DRI from the same sampling plenum. Aerosol samples were collected by DRI on the following media: Gelman (Ann Arbor, MI) polymethylpentane ringed, 2.0 µm pore size, 47 mm diameter

PTFE Teflon-membrane filters (#RPJ047) for particle mass, elements and water soluble chloride, nitrate, sulfate, ammonium; Pallflex (Putnam, CT) 47 mm diameter pre-fired quartz-fiber filters (#2500 QAT-UP) for organic and elemental carbon; and Pallflex (Putnam, CT) T60A20 102 mm diameter Teflon-impregnated glass fiber TIGF) filters followed by a cartridge of 20-60 mesh Amberlite XAD-4 (Aldrich Chemical Company, Inc.) sandwiched between two polyurethane foam (PUF) plugs for organic speciation. A 2,4-dinitrophenylhydrazine (DNPH) cartridge (Sep-Pak) sampler for carbonyl compounds, a Tenax sampler for hydrocarbons in the range of C₈ to C₂₀, and a canister sampler for C₂-C₁₂ volatile organic compound speciation were added to the sample train during light-duty passenger vehicle testing as part of the California Regional PM₁₀/PM_{2.5} Air Quality Study (CRPAQS) source characterization project.²³

PM_{2.5} mass was monitored during the dynamometer tests for all SI and CI vehicles using a tapered element oscillating microbalance (TEOM), particle light scattering with a DustTrak nephelometer, and particle absorption using a photoacoustic instrument^{24,25} to examine changes in emission rates and ratios of black carbon to PM_{2.5} with varying operating conditions.¹⁷ The continuous monitors also sampled from the same secondary dilution plenum connected to the primary dilution tunnel, both for gasoline and diesel vehicles. Continuous measurements of DustTrak light scattering provided immediate feedback about the nature of the emissions from vehicles and identified portions of the driving cycles where particulate emissions are greatest and least. They were also useful in determining whether the dilution tunnel had been adequately flushed between measurements. The continuous data were time-averaged and accumulated (in real-time) to provide total black carbon emissions and total particle emissions for use in comparison to the elemental carbon data from Thermal/Optical carbon analysis of the quartz filter and gravimetric mass analysis of the Teflon filters.

Periodic dynamic blank samples were collected during both phases of the vehicle testing program to characterize the dilution air used in BKI's constant volume dilution system (PDP-CVS) and in the combined WVU primary dilution system and DRI secondary dilution sampler. The blanks also characterize any sampling artifacts that may have been introduced by components of the sampling system. The methods used to collect these blanks were identical to that used for the vehicle exhaust samples except that no vehicle dynamometer test was run. The use of dynamic blanks for subtracting background contributions is not straightforward with

regard to development of source composition profiles that include organic carbon and speciated organic compounds. Examination of the continuous light scattering and adsorption data for three of the SI dynamic blanks indicates that residual levels drop off rapidly and do not strongly influence the average concentration of the hour-long blank samples. Similar results were obtained for the CI dynamic blanks. We note that the primary dilution air was HEPA filtered to remove atmospheric background. Some of the organic carbon in the blanks may be an artifact of SVOCs desorbing off the walls of the sampling system and adsorbing on the quartz filter. Desorption of SVOCs is favored in the equilibrium process of passing clean dilution air through the sampling system. Furthermore, subtracting the dynamic blank concentrations of PAHs essentially eliminates the heavier PAHs from the speciation profile for many of the low-emitting, late model low mileage SI vehicles and lower emitting CI vehicles. Additionally, many of the PAHs with positive values have large relative uncertainties. Based upon these considerations, the profiles developed by DRI for study for subsequent receptor model calculations are reported here without dilution tunnel blank corrections. However, all samples were corrected for field/transport blanks. Results for the dilution tunnel blanks are provided in the supplemental information section.

Analytical Methods

Prior to use, sampling media were pre-cleaned as follows: quartz fiber filters were baked for several hours in a muffle furnace at 900°C, and TIGF filters were cleaned by sonication for 10 minutes in dichloromethane (CH_2Cl_2) twice, with the solvent replaced and drained, and sonicated for 10 minutes in methanol twice with the solvent replaced. New XAD-4 was washed with liquinox soap and rinsed with hot water, followed with DI water and technical grade methanol (3-4 times). The XAD-4 was then extracted using a Dionex Accelerated Solvent Extractor (ASE) with dichloromethane (CH_2Cl_2) at 1500 psi and 80°C, followed by acetone. It was then dried in a vacuum oven at 50°C, and stored in clean 1L glass jars that were placed in aluminum cans with activated charcoal. PUF plugs were cleaned by first washing with distilled water, followed by Dionex ASE extraction for 15min/cell with acetone at 1500 psi and 80°C, followed by 10% diethyl ether in hexane under the same conditions. The extracted PUF plugs were dried in a vacuum oven at 50°C for approximately 3 days or until no solvent odor was detected, and stored in clean 1L glass jars with Teflon-lined lids wrapped in aluminum foil. Each batch of

precleaned XAD-4 resin and ~10% of precleaned TIGF filters and PUF plugs were checked for purity by solvent extraction and GC/MS analysis of the extracts. The PUF plugs and XAD-4 resins were assembled into glass cartridges (10 g of XAD between two PUF plugs) and stored at room temperature prior to shipment to the field. All samples were shipped back to DRI in coolers at approximately 4°C and stored in a freezer prior to extraction.

Weighing was performed on a Cahn 31 electro microbalance with ± 0.001 mg sensitivity. Unexposed and exposed Teflon-membrane filters were equilibrated at a temperature of 20 ± 5 °C and a relative humidity of $30 \pm 5\%$ for a minimum of 24 hours prior to weighing. The charge on each filter is neutralized by exposure to a polonium source for 30 seconds prior to the filter being placed on the balance pan. X-ray fluorescence (XRF) analysis was performed on Teflon-membrane filters for elemental analysis using a Kevex Corporation Model 700/8000 energy dispersive x-ray fluorescence (EDXRF) analyzer.²⁶ Chloride (Cl^-), nitrate (NO_3^-), and sulfate (SO_4^{2-}) ions were measured with the Dionex 2020i (Sunnyvale, CA) ion chromatograph (IC). The Dionex system contains a guard column (AG4a column, Cat. No. #37042) and an anion separator column (AS4a column, Cat. No. #37041) with a strong basic anion exchange resin, and an anion micro membrane suppressor column (250' 6 mm ID) with a strong acid ion exchange resin. The anion eluent consists of sodium carbonate (Na_2CO_3) and sodium bicarbonate (NaHCO_3) prepared in distilled, deionized water. A Technicon (Tarrytown, NY) TRAACS 800 Automated Colorimetric System (AC) was used to measure ammonium concentrations by the indolphenol method.

Elemental carbon (EC) and organic carbon (OC) were measured by thermal optical reflectance (TOR) method using the IMPROVE (Interagency Monitoring of Protected Visual Environments) temperature/oxygen cycle (IMPROVE TOR).^{27, 28} Samples were also analyzed according to the Speciation Trends Network (STN) Protocol using a thermal/optical transmittance (TOT) instrument (29). In both methods, samples are collected on quartz filters. A section of the filter sample is placed in the carbon analyzer oven such that the optical reflectance or transmittance of He-Ne laser light (632.8 nm) can be monitored during the analysis process. The filter is first heated under oxygen-free helium purge gas. The volatilized or pyrolyzed carbonaceous gases are carried by the purge gas to the oxidizer catalyst where all carbon compounds are converted to carbon dioxide. The CO_2 is then reduced to methane, which is

quantified by a flame ionization detector (FID). The carbon evolved during the oxygen-free heating stage is defined as “organic carbon”. The sample is then heated in the presence of helium gas containing 2 percent of oxygen and the carbon evolved during this stage is defined as “elemental carbon”. Some organic compounds pyrolyze when heated during the oxygen-free stage of the analysis and produce additional EC, which is defined as pyrolyzed carbon (PC). The formation of PC is monitored during the analysis by the sample reflectance or transmittance. EC and OC are thus distinguished based upon the refractory properties of EC using a thermal evolution carbon analyzer with optical (reflectance or transmittance) correction to compensate for the pyrolysis (charring) of OC. Carbon fractions in the IMPROVE method correspond to temperature steps of 120°C (OC1), 250°C (OC2), 450°C (OC3), and 550°C (OC4) in a nonoxidizing helium atmosphere, and at 550°C (EC1), 700°C (EC2), and 850°C (EC3) in an oxidizing atmosphere. The temperature steps in the STN thermal evolution protocol are 310°C, 480°C, 615°C, and 900°C in a nonoxidizing helium atmosphere and 600°C, 675°C and 825°C, in an oxidizing atmosphere. The STN method uses fixed hold times of 45 to 120 seconds at each heating stage and IMPROVE method uses variable hold times of 150-580 seconds so that carbon responses return to baseline values.

Thermal optical analysis of ambient samples by IMPROVE and STN protocols generally yield equivalent total carbon but STN EC is often less than IMPROVE EC.^{30, 31} Because EC and OC are operationally defined by the method, the specific instrument used, details of its operation, and choice of thermal evolution protocol can influence the split between EC and OC.^{32,33} Visual examination of filter darkening at different temperature stages have shown that substantial charring takes place within the filter, possibly due to adsorbed organic gases or diffusion of vaporized particles. The filter transmittance is more influenced by within-filter charring, whereas the filter reflectance is dominated by charring of the near-surface deposit. TOR and TOT corrections converge in the case of only a shallow surface deposit of EC or only a uniformly distributed pyrolyzed organic carbon (POC) through the filter and diverge when EC and POC exist concurrently at the surface and are distributed throughout the filter, respectively, especially when the surface EC evolves prior to the POC. The difference between TOR and TOT partly depends on the POC/EC ratio in the sample.³⁰ Thus, highly loaded source samples would yield similar EC values for TOR and TOT corrections, while lightly loaded source and ambient samples would typically yield different EC values. While EC values for TOR may tend toward

higher EC due to underestimation of the POC correction, higher absorption efficiency of POC within the filter may tend toward lower EC values for TOT.

For organic compound speciation, PUF/XAD/PUF cartridges and TIGF filters were extracted and analyzed together, except for CI blanks, idle cycle tests and selected samples with low PM loadings, which were extracted and analyzed separately. Prior to extraction, the following deuterated internal standards were added to each filter and cartridge pair: naphthalene-d₈, acenaphthylene-d₈, phenanthrene-d₁₀, anthracene-d₁₀, chrysene-d₁₂, pyrene-d₁₀, benz[a]anthracene-d₁₂, benzo[a]pyrene-d₁₂, benzo[e]pyrene-d₁₂, benzo[k]fluoranthene-d₁₂, benzo[g,h,i]perylene-d₁₂, coronene-d₁₂, cholestane-d₅₀, and tetrocosane-d₅₀. Filters and XAD-4 were extracted with dichloromethane, followed by acetone, using the Dionex ASE. Since PUF media degrade when extracted with dichloromethane, the PUF were extracted twice with acetone using the Dionex ASE. The extracts were then combined and concentrated by rotary evaporation at 20 °C under gentle vacuum to ~1 ml and filtered through 0.45 mm Acrodiscs (Gelman Scientific). The extract was concentrated to 1 ml and split into two fractions: (1) the first fraction was precleaned by the solid-phase extraction technique using Superclean LC-SI SPE cartridges (Supelco) with sequential elution with hexane, and hexane/benzene (1:1).^{34, 35} The hexane fraction contained the non-polar aliphatic hydrocarbons, and hopanes and steranes, and the hexane/benzene fraction contained the PAH. These two fractions were combined and concentrated to ~100 µL and analyzed by GC/MS technique for hydrocarbons, hopanes, steranes, PAH and oxy-PAH. The second fraction was utilized for the polar compound analysis without precleaning. It was derivatized using a mixture of bis(trimethylsilyl)trifluoroacetamide and pyridine to convert the polar compounds into their trimethylsilyl derivatives. The second fraction was evaporated to 100 µl under moisture filtered ultra high purity nitrogen and transferred to 300 µl silanized glass inserts (National Scientific Company, Inc.). Samples were further evaporated to 50 µl, and 25 µl of pyridine (Pierce), 25 µl of internal standard mixture (succinic acid d-4, myristic acid -d₂₇, and 1,2,4-butanetriol), and 150 µl of BSTFA with 1 % TMCS [N, O-bis(trimethylsilyl) trifluoroacetamide with 1% trimethylchlorosilane (Pierce)] were added. The glass insert containing the sample was put into a 2 ml vial and sealed. The sample was then placed into a thermal plate (custom made) containing individual vial wells at 70 °C for 3 hours. The calibration solutions were freshly prepared and derivatized just prior to the analysis of each

sample set, and then all samples were analyzed by GC/MS within 18 hours to avoid degradation. Analysis of the polar organic compounds and the internal standards added are described elsewhere.^{36, 37}

Samples were analyzed by gas chromatography/mass spectrometry (GC/MS), using Varian CP-3800 GC equipped with a CP8400 autosampler and interfaced to a Varian Saturn 2000 Ion Trap operating in electron impact (EI) ionization mode (for PAH, oxy-PAH, hopanes/steranes and alkanes) or chemical ionization (CI) mode, using isobutene as an ionization gas (for polar compounds). Concentrations were quantified by comparing the response of the deuterated internal standards to the analyte of interest.¹⁰ It should be also noted that due to the lack of authentic standards, most of the hopanes/steranes are identified tentatively (with exception of hop19, hop23 and ster45, for which standards were available), based on the available literature data.^{34,35,38-40} Diesel fuel and gasoline and diesel lubrication oil samples were obtained from the vehicles immediately after emissions sampling and were analyzed for PAH and hopanes/steranes. The fuel and oils were cleaned and fractionated prior to analysis using the method described by Wang, et al.^{34, 35} and detailed elsewhere.¹⁰

RESULTS

The 30 SI and 8 CI individual or analytical composite samples were further combined into six composite SI and four composite CI exhaust profiles as shown in Table 3. The SI composite profiles consist of low and high emitters for both “cold” (SI_LC and SI_HC, respectively) and “warm” (SI_LW and SI_HW) emission tests. Incremental cold start profiles were obtained by subtracting the warm samples from the corresponding cold samples, but the analytical uncertainties are too high for them to be useful in receptor modeling. A separate pair of composite profiles was also derived for vehicles with higher proportions of elemental carbon (SI_BC and SI_BW). MDD is the composite of all available speciation data for light-heavy and medium-heavy trucks. HCS and HW are composites exhaust profiles for heavy-heavy trucks on the City Suburban Heavy Vehicle Route and Highway Driving Cycles, respectively. HDD is the composite of the HCS and HW profiles. In several tests, secondary dilution of diesel exhaust resulted in insufficient amounts of sample for quantitative analysis of many organic species. These samples were excluded from the composite profiles. Samples collected for idle tests were

all below detection. The composite profiles combine samples with similar PM_{2.5} emission rates, EC/TC ratios, and abundances of hopanes, steranes and three of the high-molecular weight PAHs, benzo(ghi)perylene, indeno(1,2,3-cd)pyrene and coronene, that are potential markers for SI exhaust. The speciated emission rates are listed for the composite profiles in Table S3, located in the supplemental information section. These profiles were subsequently used in CMB receptor modeling to estimate the relative contributions of SI and CI exhaust to ambient carbonaceous particles in California's South Coast Air Basin.¹⁸

Fine Particle Mass, Ions and Metals

The average PM_{2.5} emission rates for SI vehicles on the UDC were 27.2 mg/mile (251.9 maximum) for cold start tests and 16.9 mg/mile (207.9 maximum) for warm start tests. The distribution of PM_{2.5} emissions for the 57 test SI vehicles is highly skewed with 10 percent that were the highest emitters accounting for 62 and 69 percent of the cumulative emissions for cold and warm tests, respectively. Average PM_{2.5} emission rates for heavy-duty trucks were 404 mg/mile (1125 maximum) on the hot city-suburban route cycle and 187 mg/mile (520 maximum) on the highway cycle. The distribution of PM_{2.5} emissions for heavy-duty trucks is less skewed than light-duty SI vehicles with 12 percent of the trucks accounting for 30 percent of the cumulative emissions for the hot CSHVR cycle.

The fractions of non-carbonaceous species to the total PM_{2.5} in the composite profiles were negligible for both spark-ignition and diesel vehicles. Silicon and ammonium sulfate were dominant in the samples for light-duty vehicles in groups 1-4. Since these are major constituents of the ambient atmospheric PM, they are likely entrained through the vehicle's air filter. Zinc, calcium, and phosphorus, which are the dominant elements in lubricating oil, were present in all samples. The emission rates of these elements for SI vehicles, shown in Figure 1a, are highly variable with a range spanning nearly three orders of magnitude (maximum of 11.8 and minimum of 0.015 mg/mi). However, the relative proportions were constant, indicating that lubrication oil is likely the common source of these elements. The emissions distribution was highly skewed with most 1990 and newer SI vehicles emitting less than 0.1 mg/mile of the three elements and most pre-1990 SI vehicles showing higher emissions. The range of emission rates of these elements was not as large for CI exhaust (Figure 1b). The lower range was comparable

to pre-1990 SI vehicles and the upper end was comparable to the highest emitting SI vehicles. The relative emissions of the three elements were more variable in CI exhaust with lower proportional amounts of phosphorus with increasing emissions. While there is a general tendency toward higher $PM_{2.5}$ emissions with greater emissions of zinc, calcium and phosphorus, the correlations were weak.

Carbon Composition

Over half the mass of carbonaceous particles emitted by heavy-duty diesel trucks is elemental carbon, as illustrated in Figure 2. The EC/TC ratios for the combined light and medium heavy-duty diesel trucks (MDD) and the heavy heavy-duty diesel trucks (HDD) were both 0.62 (IMPROVE TOR method) with about two-thirds of the EC in the EC2 fraction. By comparison, the EC/TC ratios among the SI composite profiles were lower and more variable. $PM_{2.5}$ emissions from SI vehicles with higher emission levels contain predominantly OC with EC/TC ratios of 0.17 and 0.12 for cold and warm start tests, respectively. The EC/TC ratios for lower emitters were 0.31 for both cold and warm start tests. SI vehicles emitted a larger fraction of EC as EC1 than CI vehicles. Table 3 shows that there were a few moderate to high-emitting SI vehicles with EC/TC ratios that were comparable to heavy-duty diesel trucks (0.56 for cold start test and 0.53 for warm start test) with higher fractions of EC in the EC2 fraction.

EC and OC are operationally defined parameters and may vary with the specific instrument and protocol used. The scatterplots in Figure 3 for TC and EC show that measurements by the IMPROVE TOR and STN TOT protocols agree well for highly loaded samples. However, the STN TOT/IMPROVE TOR ratios for EC decrease with decreasing sample loadings. The divergence between the two methods occurs for lightly loaded SI samples. Figure 4 shows scatterplots of STN versus IMPROVE EC measurements for all CI (top left) and for SI (top right) samples. The same two plots are shown for lower exhaust concentrations in the bottom panels. While the two methods agree for CI samples for the entire range of exhaust concentrations, IMPROVE TOR EC is higher relatively to STN TOT EC in SI samples at lower exhaust concentrations. The effect of variations in EC measurements by the two methods on the CMB source apportionments is discussed elsewhere.¹⁸

The continuous photoacoustic light absorption measurements showed that all vehicles tested, including late model spark ignition vehicles, had black carbon emissions.¹⁷ For SI vehicles, black carbon and PM_{2.5} emission rates can be two to eight times larger during the cold start phase than during hot stabilized operation. Relatively clean spark ignition vehicles have black carbon emissions that occur during the more aggressive portions of the driving cycle, with maximum emissions typical during cold start and a secondary peak during aggressive acceleration, which are both associated with fuel/air ratio enrichment. Figure 5 shows examples of the variations in light absorption during the test cycle for very clean, normal, and visibly smoking SI vehicles, and a light-duty diesel vehicle. The ‘clean’ and ‘normal’ vehicles had greatest emission concentrations in the first 5 minutes of phase 1 (cold start), and the similar driving cycle after 35 minutes in the phase 3 warm start produced much lower emissions. Virtually all of the PM emissions from “normal emitters” come from the first few minutes during a cold start and from hard accelerations with relatively higher amounts of black carbon produced during both cold starts and hard accelerations.

Distribution of Organic Compounds in Exhaust and Lubricating Oil

Figure 6 presents the emission rates (µg/mile) of higher molecular-weight polycyclic aromatic hydrocarbons (PAH) that are mostly particle-associated in the composite diesel and gasoline exhaust. Gasoline vehicle exhaust contains higher proportions of the 6-and 7-ring PAH, indeno[1,2,3-cd]pyrene, benzo[ghi]perylene and coronene in comparison with diesel exhaust. This is consistent with the comparative composition of PAH emissions that have been reported in previous studies.^{10, 41} In contrast, diesel emissions are enriched in 2- to 4-ring semi-volatile PAHs, including primarily particle-associated chrysene and benz(a)anthracene. Benz(a)anthracene is relatively reactive PAH, thus it is not a suitable tracer for diesel emissions. However, chrysene is a stable PAH and is mostly particle associated at ambient conditions. Chrysene correlates well with IMPROVE TOR EC for the four composite diesel profiles ($r^2=0.97$).

While several 6 and 7-ring PAH are potential markers for gasoline exhaust, their relative abundances to total carbon emissions were variable. PAHs in lubricating oils may be one possible explanation of this variability. In a previous study, we reported that these PAHs are

found in used gasoline motor oil but not in fresh oil and are negligible in used diesel engine oil.¹⁰ Combustion-produced PAH can escape from the combustion chamber past the piston rings with the blow-by gases that can absorb into the crankcase oil. We postulate that the concentration of PAH in the lubrication oil increases with mileage accumulation until the next oil change. Consequently, emissions of PAH may also depend on the rate of consumption and age of the lubrication oil as well as the vehicle operating conditions that directly produce PAHs during combustion. Figure 7 shows the concentrations of the same eight higher molecular weight PAHs in diesel fuel and diesel and gasoline vehicle lubrication oils (in $\mu\text{g/g}$). Gasoline lubrication oils contain higher concentrations of these PAH in comparison with diesel fuels or oils. This is consistent with previous results.¹⁰ Note that while the absolute concentrations of PAHs vary in the gasoline vehicle lubricating oil, their proportions to each other are consistent.

Hopanes and steranes are compounds present in crude oil as a result of the decomposition of sterols and other biomass.³⁹ These compounds are present in lubricating oils, but not in the fuels.¹⁰ They have been used as molecular markers for vehicle emissions and are higher in vehicles that emit oil.^{10, 38-40} Figure 8 shows the emission rates of individual hopanes and steranes for the composite diesel and gasoline vehicle profiles. Table S3 explains the mnemonics. CI composite exhaust profiles contain higher amounts of lower molecular weight hopanes and steranes, while the SI exhaust profiles have a more even distribution by molecular weight. This result is inconsistent with previous studies that have shown similar composition of hopanes and steranes in SI and CI exhaust.¹⁰ As noted earlier, the results for most CI vehicle samples have higher uncertainty due to the higher dilution ratios used in sample collection. Some CI samples have the expected patterns of hopanes and steranes, but were not included in the composite profile due to invalid analytical results for other species (e.g., invalid carbon data due to overloaded quartz filter).

Figure 9 shows the comparison of hopanes and steranes profiles in the lubricating oils and in the CI and SI vehicle exhaust. The composition of steranes and hopanes are similar in SI vehicle exhaust to that in lubrication oil, especially for steranes. Thus, we estimate lubricating oil emission rates for SI vehicles by assuming that all steranes present in emissions are from the lubrication oil and are not destroyed during the combustion process. The lubrication oil emission rates (Oil Em) were calculated from the following equation:

$$\text{Oil Em (g/mile)} = S_{\text{em}} (\mu\text{g/mile})/S_{\text{oil}} (\mu\text{g/g}) \quad (1)$$

where S_{em} is total steranes emission rate from the SI vehicles and S_{oil} is the total concentration of steranes in the lubrication oil of the corresponding vehicle. The emissions of PAHs that originate from the lubrication oil can be estimated from equation (2):

$$\text{PAH emitted with oil } (\mu\text{g/mile}) = \text{PAH}_{\text{oil}} (\mu\text{g/g}) * \text{Oil Em (g/mile)} \quad (2)$$

The ratio of PAHs originating from the oil to total PAHs in the exhaust gives the fraction of PAH in the emissions that are associated with oil. Table 4 shows the results calculated for the same eight and three (indeno[1,2,3-cd]pyrene, benzo[ghi]perylene and coronene) higher mw PAH, for SI vehicles. The contribution of lubrication oil to emissions of PAHs ranges from 0.2% to 79% and from 0.1% to 55% for eight and three PAHs, respectively. This contribution depends upon two key factors: (1) the vehicle's oil consumption rate; and (2) time and mileage since the oil was last changed. For example, two SI vehicles from category 7 (SI_7C2 and SI_7C3) are not the highest lubrication oil emitters (67 and 96 mg/mile, respectively, as compared to over 300 mg/mile for vehicle SI_10C3), but the PAH contributions from the lubrication oil are the highest among the SI group. This suggests that these two vehicles are excessive oil emitters. Indeed, the OC/TC ratio is also the highest for these two vehicles (91 and 93%, IMPROVE method). The highest lubrication oil emitter, vehicle SI_10C3 (358 mg/mile) has only moderate contribution of heavy PAH from the lubrication oil (5% for three PAH) but its lubrication oil was only 8 days old and the concentrations of these PAH in the oil were relatively low (See Figure 7). Vehicles from category 10 are high PM emitters, but the PAHs in the exhaust are formed mostly during the combustion process with a relatively minor contribution from the lubrication oil. It should be noted that the lubrication oil emissions calculated according to the equation (1) are often higher than the $\text{PM}_{2.5}$ emissions. However, not all components of burned oil are in particulate matter as some may be too volatile to condense on the particles or may be destroyed during the combustion process.

Aliphatic and cyclic hydrocarbons were measured in vehicle emissions only. We quantified 15 n-alkanes (from C14 to C28), 5 branched alkanes: norfarnesane (2,6,10-trimethylundecane), farnesane (2,6,10-trimethyldodecane), norpristane (2,6,10-trimethylpentadecane), pristane (2,6,10,14-tetramethylpentadecane), phytane (2,6,10,14-

tetramethylhexadecane), and 14 n-alkylcyclohexanes (from C7- to C20-cyclohexane). Table S-3 lists the emission rates of these alkanes and, in addition, a sum of n-alkylcyclohexanes for composite CI and SI vehicles. It is clear from this table that the emission rates of these compounds are much higher for CI than SI vehicles. In fact, only high-emitting SI vehicles, especially in hot start mode, emit any significant amounts of branched and cyclic hydrocarbons. This is true for n-alkanes as well. For CI vehicle exhaust, n-alkanes, branched alkanes and n-alkylcyclohexanes constitute approximately 60-80%, 6-20% and 6-30%, respectively, of total aliphatic and cyclic hydrocarbons. For SI vehicles, these percentages are more spread out, but for the higher emitting vehicles, they are in the same range. All five branched alkanes are present in the spark ignition high-emitting cold and warm (SI_HC and SI_HW) profiles as well; thus they are not unique tracers for diesel vehicle exhaust.

Polar compounds were measured in the vehicle emissions only. Table S-3 lists the emission rates of several polar compounds: tridecanoic acid (alkanoic acid), succinic and glutaric acid (alkanedioic acids), maleic acid (alkenedioic acid), phthalic and isophthalic acid (aromatic diacid). The emission rates of these compounds are much higher for CI than SI vehicles. It is interesting to note that diacids that are often considered as atmospheric transformation products are emitted by CI vehicles.⁴³⁻⁴⁸ Thus, these compounds are not unique tracers for either vehicle exhaust or secondary organic aerosols.

DISCUSSION

The results of this study are generally consistent with other recent vehicle exhaust emission characterization studies.^{4-7, 10,11} PM emissions of most SI vehicles were relatively low compared to CI vehicles, especially in hot-stabilized mode. The PM_{2.5} emissions of some SI high emitters were comparable to the emissions of most CI vehicles on the Highway Test Cycle. Organic carbon and elemental carbon are the most abundant species in motor vehicle exhaust, accounting for over 95% of the total PM_{2.5} mass. Elemental carbon is dominant in diesel exhaust and its proportion to total carbon is generally less at lower engine load. Over half the mass of carbonaceous particles emitted by heavy-duty diesel trucks is EC measured by IMPROVE TOR with about two-thirds in the EC₂ fraction. PM_{2.5} emissions from SI high-emitters contain predominantly OC. However, black carbon and PM emission rates for SI vehicles can be two to

eight times larger during the cold start phase than during hot stabilized operation, which confirm previous results from NRFAQS.^{5,6} Relatively clean SI vehicles can also produce black carbon emissions during the more aggressive portions of the driving cycle. Therefore, the emission profiles for clean SI vehicles from dynamometer tests may contain higher fractions of EC than would be produced in congested urban driving conditions. There are a few moderate to high-emitting SI vehicles with EC/TC ratios that are comparable to heavy-duty diesel trucks with higher fractions of elemental carbon in the EC2 fraction.

Total carbon measurements by the IMPROVE-TOR and STN-TOT protocols agree well for diesel exhaust samples. EC emission rates measured by IMPROVE were also in good agreement with STN for CI exhaust. While EC measurements for SI vehicles agreed between the two protocols at higher PM emission rates, the divergence increased with decreasing PM emissions. Using IMPROVE EC rather than STN EC in the Chemical Mass Balance fit for the Gasoline/Diesel PM Split Study resulted in about 40 percent higher CI contributions to ambient particulate carbon, but was not statistically significant within two overlapping standard errors.¹⁸ However, these results were attributed to greater differences between the two carbon analysis protocols for ambient samples.¹⁸

SI vehicles, whether low or high emitters, have higher emission rates than CI vehicles (per travel distance basis) of the high molecular-weight particulate PAHs, benzo(ghi)perylene, indeno(1,2,3-cd)pyrene, and coronene. Diesel vehicles have higher emissions of 2 to 4-ring semi-volatile PAHs. Hopanes and steranes are present in lubricating oil with similar composition for both gasoline and diesel vehicles and are negligible in gasoline or diesel fuels. CI vehicles emitted greater total amounts on a mass per mile basis, but abundances were comparable to SI exhaust normalized to total carbon emissions within margin of error. Emission rates of hopanes and steranes are the highest for both gasoline and diesel “high emitting” vehicles. Diacids were emitted by CI vehicles, and cannot be considered unique tracers for either vehicle exhaust or secondary organic aerosols.

We also confirmed that the high molecular-weight particulate PAHs, benzo(ghi)perylene, ideno(1,2,3-cd)pyrene, and coronene, are found in used gasoline motor oil, but not in fresh oil, and are negligible in used diesel engine oil.¹⁰ The contributions of

lubrication oils to abundances of these PAHs in the exhaust were large in some cases and were variable with the age and consumption rate of the oil. These factors contributed to the observed variations in their abundances to total carbon or PM_{2.5} among the SI composition profiles obtained in this study. As in the NFRAQS, we found in this study that the CMB apportionments of SI exhaust were sensitive to the abundance of high-molecular weight PAHs in the profile and to a lesser extent to hopanes and steranes.¹⁸ Variations in abundances of these species in SI and CI exhaust profiles and differences in IMPROVE and STN EC measurements were two of the more important sources of uncertainty in the CMB analysis for this study.¹⁸

ACKNOWLEDGMENTS

This study was funded by the National Renewable Energy Laboratory through the U.S. Department of Energy's Office of FreedomCAR and Vehicle Technologies. We acknowledge the vehicle emissions tests performed by Bevilacqua Knight Incorporated and West Virginia University. We also acknowledge the following DRI personnel for their assistance: Kelly Fitch for field sampling, Mark McDaniel and Anna Cunningham for the organic speciation analysis, and Steven Kohl, Barbara Hinsvark and Dale Crow for analysis of inorganic species. We are grateful to Ralphs Grocery for providing a test site and test vehicles. We also thank John Watson for his comments on the manuscript and valuable scientific discussions.

SUPPORTING INFORMATION AVAILABLE

Table S1 displays the make, model, year, mileage and PM_{2.5} emission rate of each SI vehicle as well as the analytical compositing scheme for composition profiles. Table S2 displays similar information for the CI vehicles. Table S3 lists the speciated emission rates for the composite SI and CI exhaust profiles. A discussion of data quality is presented along with analysis of the dilution tunnel samples. Figure S1 compares PM_{2.5} emission rates determined by EPA/BKI and UWV from their primary dilution tunnel versus the corresponding values obtained by DRI from the secondary dilution tunnel sampler. Figure S2 show correlation plots of gravimetric mass vs. sum of elements by XRF, ions by IC and AA, and carbon by TOR for SI and CI vehicles. Table S4 displays the mass loadings in the tunnel blanks relative to the composite SI and CI exhaust

samples. Data and project reports from the study are available online at the following web site:

http://www.nrel.gov/vehiclesandfuels/nfti/feat_split_study.html

REFERENCES

1. Janssen, N.A.; Swartz, J.; Zanobetti, A.; Suh, H.H. Air Conditioning and Source-Specific Particles as Modifiers of the Effect of PM(10) on Hospital Admissions for Heart and Lung Disease. *Environ. Health Perspect.*, **2002**, 110, 43-49.
2. Laden, F.; Neas, L.M.; Dockery, D.W.; Schwartz, J. Association of Fine Particulate Matter from Different Sources with Daily Mortality in Six U.S. Cities. *Environ. Health Perspect.*, **2000**, 108, 941-947.
3. Schauer J.J.; Rogge W.F.; Mazurek M.A.; Hildemann L.M.; Cass G.R.; Simoneit B.R.T. Source apportionment of airborne particulate matter using organic compounds as tracers. *Atmos. Environ.* **1996**, 30, 3837-3855.
4. Sagebiel, J.C.; Zielinska, B.; Walsh, P.A.; Chow, J.C.; Cadle, S.H.; Mulawa, P.; Knapp, K.T.; Zweidinger R.B; Snow, R. PM-10 Exhaust Samples Collected During IM-240 Dynamometer Tests of In-Service Vehicles in Nevada. *Environ. Sci. Technol.*, **1997**, **31**:75-83.
5. Watson, J.; Fujita, E.; Chow, J.C.; Zielinska, B.; Richards, L.; Neff, W.; Dietrich, D. Northern Front Range Air Quality Study. Final report prepared for Colorado State University, Fort Collins, CO, July 1998.
6. Fujita, E.; Watson, J.G.; Chow, J.C.; Robinson, N.; Richards, L.; Kumar, N. Northern Front Range Air Quality Study. Volume C: Source Apportionment and Simulation Methods and Evaluation. Final report prepared for Colorado State University, Fort Collins, CO, July 1998.
7. Zielinska, B.; McDonald, J.; Hayes, T.; Chow, J.C.; Fujita, E.M.; Watson J.G. Northern Front Range Air Quality Study, Volume B: Source Measurements. Final report prepared for Colorado State University, Fort Collins, CO, and Electric Power Research Institute, Palo Alto, CA, by Desert Research Institute, Reno, NV, July 1998.
8. Schauer, J.J.; Kleeman, M.J.; Cass, G.R.; Simoneit B.R.T. Measurement of Emission from Air Pollution Sources. 3. C1-through C-30 Organic Compounds from Medium Duty Diesel Trucks. *Environ Sci Technol.*, **1999**, 33: 1578-1587.
9. Schauer, J.J.; Kleeman, M.J.; Cass, G.R.; Simoneit B.R.T. Measurement of Emission from Air Pollution Sources. 5. C1-through C-30 Organic Compounds from Gasoline-Powered Motor Vehicles. *Environ Sci Technol.* **2002**, 36: 1169-1180.

- 661 10. Zielinska, B.; Sagebiel, J.; McDonald, J.D.; Whitney K.; Lawson D.R. Emission Rates
662 and Comparative Chemical Composition from Selected In-Use Diesel and Gasoline-
663 Fueled Vehicles. *J. Air & Waste Manage. Assoc.* **2004**, 54:1138-1150.

- 664 11. Zielinska, B.; Sagebiel, J.C.; Arnott, W.P.; Rogers, C.F.; Kelly, K.E.; Wagner, D.A.;
665 Lightly, J.S.; Sarofim, A.F.; Palmer, G. Phase and Size Distribution of Polycyclic
666 Aromatic Hydrocarbons in Diesel and Gasoline Vehicle Emissions. *Environ. Sci.*
667 *Technol.* **2004**, 38, 2557-2567.

- 668 12. Lev-On, M.; LeTavec, C.; Uihlein, J.; Kimura, K.; Alleman, T. L.; Lawson, D. R.;
669 Vertin, K.; Thompson, G. J.; Clark, N.; Gautam, M.; Wayne, S.; Okamoto, R.; Rieger, P.;
670 Yee, G.; Zielinska, B.; Sagebiel, J.; Chatterjee, S.; Hallstrom K. Chemical Speciation of
671 Exhaust Emissions from Trucks and Buses Fueled on Ultra-Low Sulfur Diesel and CNG.
672 SAE Technical Paper 2002-01-0432.

- 673 13. Maricq, M.M.; Podsiadlik, D.H.; Chase, R.E. Examination of the Size-Resolved and
674 Transient Nature of Motor Vehicle Particle Emissions. *Environ. Sci. Technol.* **1999**, 33,
675 1618-1628.

- 676 14. Cadle, S.H.; Mulawa, P.; Groblicki, P.; Laroo, C.; Ragazzi, R.; Nelson, K.; Gallagher G.;
677 Zielinska, B. In-Use Light-Duty Gasoline Vehicle Particulate Matter Emissions on Three
678 Driving Cycles. *Environ. Sci. Technol.*, **2001**, 35, 26-32.

- 679 15. Cadle, S.H.; Mulawa, P.; Ball, J.; Donase, C.; Weibel, A.; Sagebiel, J.C.; Knapp, K.T.;
680 and Snow, R. (1997) Particulate emission rates from in-use high-emitting vehicles
681 recruited in Orange County, California. *Environ. Sci. Technol.*, **31**:3405-3412.

- 682 16. Mazzoleni, C.; Moosmüller, H.; Kuhns, H.D.; Keislar, R.E.; Barber, P.W.; Nikolic, D.;
683 Nussbaum, N.J.; Watson, J.G. Correlation Between Automotive CO, HC, NO, and PM
684 Emission Factors from On-road Remote Sensing: Implications for Inspection and
685 Maintenance Programs. *Transport. Res.* **2004**, D9, 477-496.

- 686 17. Fujita, E.M.; Zielinska, B.; Arnott, W.P.; Campbell, D.E.; Rinehart, L.; Sagebiel, J.C.;
687 Chow J.C. Gasoline/Diesel PM Split Study: Source and Ambient Sampling, Chemical
688 Analysis, and Apportionment Phase. Final report submitted to the U.S. Department of
689 Energy National Renewable Energy Laboratory, Golden, CO, January 19, 2006.

- 690 18. Fujita, E.M.; Campbell D.E.; Arnott W.P.; Chow, J.C; Zielinska B. Evaluations of source
691 apportionment methods for determining contributions of gasoline and diesel exhaust to
692 ambient carbonaceous aerosols. *J Air Waste Manage Assoc*, in press.

- 693 19. Gabele, P. Support of the Gasoline/Diesel Particulate Matter Split Study. Final report
694 submitted by U.S. Environmental Protection Agency to Department of Energy through
695 Interagency Agreement (IAG) No. DE-AI04-2001AL67138, March 17, **2003**.

- 696 20. Clark N.N.; Wayne, W.S.; Nine, R.D.; Buffamonte, T.; Hall, T.; Rapp, B.L.; Ehompson,
697 G.; and Lyons D.W. Emissions from Diesel-Fueled, Heavy-Duty Vehicles in Southern
698 California, 2003 SAE Transaction:Journal of Fuels & Lubricants, pp.1688-1699.
- 699 21. Chang, M.C.; Yi, S.M.; Hopke, P.K.; England, G.C.; Chow, J.C.; Watson, J.G.
700 Measurement of Ultrafine Particle Size Distributions from Coal-, Oil-, and Gas-Fired
701 Stationary Combustion Sources. *J. Air Waste Manage. Assoc.*, **2004**, 54(12), 1494-1505.
- 702 22. Hildemann, L.M.; Cass, G.R.; and Markowski, G.R. A dilution stack sampler for
703 collection of organic aerosol emissions: design, characterization and field tests. *Aerosol*
704 *Sci. Technol.*, **1989**, 10:193-204.
- 705 23. Fitz, D.R.; Chow, J.M.; Zielinska, B. Development of a Gas and Particulate Matter
706 Organic Speciation Profile Data Base. Final report prepared for San Joaquin Valleywide
707 Air Pollution Study Agency, 2003.
- 708 24. Arnott, W. P.; Moosmüller, H.; Rogers, C.F.; Jin, T.; Bruch, R. Photoacoustic
709 Spectrometer for Measuring Light Absorption by Aerosols: Instrument Description.
710 *Atmos. Environ.* **1999**, 33: 2845-2852.
- 711 25. Arnott, W. P.; Moosmüller, H.; Walker, J.W. Nitrogen dioxide and kerosene-flame soot
712 calibration of photoacoustic instruments for measurement of light absorption by aerosols.
713 *Review of Scientific Instruments*, **2000**, 71(7): 4545-4552.
- 714 26. Watson, J.G.; Chow, J.C.; Frazier, C.A. 1999: X-ray fluorescence analysis of ambient air
715 samples. Elemental Analysis of Airborne Particles, Vol. 1, Landsberger, S. and M.
716 Creatchman, Eds., Gordon and Breach Science, 67-96.
- 717 27. Chow, J.C.; Watson, J.G.; Pritchett, L.C.; Pierson, W.R.; Frazier, C.A.; Purcell, R.G.:
718 The DRI Thermal/Optical Reflectance Carbon Analysis System: Description, Evaluation
719 and Applications in U.S. Air quality Studies. *Atmos.Environ.*, **1993**, 27A, 1185-1201.
- 720 28. Chow, J.C.; Watson, J.G.; Crow, D.; Lowenthal, D.H.; Merrifield, T. Comparison of
721 IMPROVE and NIOSH Carbon Measurements. *Aerosol Sci.Technol.*, **2001**, 34, 23-34.
- 722 29. Peterson, M.R.; Richards, M.H. Thermal-optical-transmittance analysis for organic,
723 elemental, carbonate, total carbon, and OCX2 in PM2.5 by the EPA/NIOSH method, in
724 Proceedings, Symposium on Air Quality Measurement Methods and Technology-2002,
725 Winegar, E.D., Tropp, R.J., Eds.; Air & Waste Management Association: Pittsburgh, PA,
726 2002, pp. 83-1-83-19.
- 727 30. Chow J.C.; Watson, J.G.; Chen, L.W.A.; Arnott, W.P.; Moosmuller, H.; Fung, K.
728 Equivalence of Elemental Carbon by Thermal/optical Reflectance and Transmittance
729 with Different Temperature Protocol. *Environ. Sci. Technol.* **2004**, 38, 4414-4422.

- 730 31. Chen, L.-W.A.; Chow, J.C.; Watson, J.G.; Moosmüller, H.; Arnott, W.P. Modeling
731 Reflectance and Transmittance of Quartz-Fiber Filter Samples Containing Elemental
732 Carbon Particles: Implications for Thermal/Optical Analysis. *J. Aerosol Sci.* **2004**, 35(6),
733 765-780.
- 734 32. Watson, J.G.; Chow, J.C.; Chen, L.-W.A. Summary of Organic and Elemental
735 Carbon/Black Carbon Analysis Methods and Intercomparisons; *Aerosol and Air Quality*
736 *Research* **2005**, 5(1), 69-102.
- 737 33. Chow, J.C.; Watson, J.G.; Chen, L.W.A.; Paredes-Miranda, G.; Chang, M.C.; Trimble,
738 D.; Fung, K.K.; Zhang, J.; Yu, J.Z. Refining Temperature Measures in Thermal/Optical
739 Carbon Analysis. *Atmos. Chem. Physics Discussion* **2005**, 5, 4477-4505.
- 740 34. Wang, Z.; Fingas, M.; Li, K. Fractionation of a Light Crude Oil and Identification and
741 Quantification of Aliphatic, Aromatic, and Biomarker Compounds by GC-FID and GC-
742 MS, Part I. *J. of Chromatograph. Sci.*, **1994**, 32, 361-366.
- 743 35. Wang, Z.; Fingas, M.; Li, K. Fractionation of a Light Crude Oil and Identification and
744 Quantification of Aliphatic, Aromatic, and Biomarker Compounds by GC-FID and GC-
745 MS. Part II, *J. of Chromatograph. Sci.*, **1994**, 32, 367-382.
- 746 36. Rinehart, L.R.; Fujita, E.M.; Chow, J.C.; Magliano, K.; Zielinska, B. Spatial distribution
747 of PM_{2.5} associated organic compounds in central California; *Atmos. Environ.* **2006**, 40,
748 290-303.
- 749 37. El-Zanan, H.S., et al., Measurement of the Aerosol Organic Mass to Organic Carbon
750 Ratio and Chemical Characterization of Atmospheric Aerosol in Support of Atlanta
751 Health Study: Particle and Multiphase Organics. *J. Air Waste Manage. Assoc.*,
752 submitted.
- 753 38. Simoneit, B.R.T. Application of Molecular Marker Analysis to Vehicular Exhaust for
754 Source Reconciliation. *International Journal of Environmental Analytical Chemistry*,
755 **1985**, 22, 203-233
- 756 39. Rogge, W.F.; Hildemann, L.M.; Mazurek, M.A.; Cass, G.R.; Simoneit, B.R.T. Sources of
757 Fine Organic Aerosol 2. Noncatalyst and Catalyst-Equipped Automobiles and Heavy-
758 Duty Diesel Trucks. *Environ. Sci. Technol.* **1993**, 27, 636-651.
- 759 40. Fraser, M.P.; Cass, G.R.; Simoneit, B.R.T. Gas-Phase and Particle-Phase Organic
760 Compounds Emitted from Motor Vehicle Traffic in a Los Angeles Roadway Tunnel.
761 *Environ. Sci. & Technol.*, **1998**, 32, 2051 -2060.
- 762 41. Miguel, A.H.; Kirchstetter, T.W.; Harley, R.A.; Hering, S.V. On-Road Emissions of
763 Particulate Polycyclic Aromatic Hydrocarbons and Black Carbon Soot from Gasoline and
764 Diesel Vehicles. *Environ.Sci.Technol.*, **1998**, 32, 450-455.

- 765 42. Fraser, M.P.; Cass, G.R.; Simoneit, B.R.T. Particle-Phase Organic Compounds Emitted
766 from Motor Vehicle Exhaust and in Urban Atmosphere. *Atmos. Environ.*, **1999**, 33, 2715-
767 2724.
- 768 43. Chebbi, A.; Carlier, P. Carboxylic Acids in the Troposphere, Occurrence, Sources, and
769 Sinks: A Review. *Atmos. Environ.* **1996**, 30, 4233-4249.
- 770 44. Grosjean, D., Seinfeld, J.H., 1989. Parameterization of the formation potential of
771 secondary organic aerosols. *Atmos. Environ.*, 23, 1733-1747.
- 772 45. Kawamura, K.; Gagosian, R.B. Implications of Omega-Oxocarboxylic Acids in the
773 Remote Marine Atmosphere for Photooxidation of Unsaturated Fatty-Acids. *Nature*,
774 **1987**, 325, 330-332.
- 775 46. Kawamura, K.; Kasukabe, H.; Barrie, L.A.. Source and Reaction Pathways of
776 Dicarboxylic Acids, Ketoacids and Dicarboxyls in Arctic Aerosols: One Year of
777 Observations. *Atmos. Environ.*, **1996**, 30, 1709-1722.
- 778 47. Keywood, M.D.; Kroll, J. H.; Varutbangkul, V.; Bahreini, R.; Flagan, R. C.; Seinfeld,
779 J.H.. Secondary Organic Aerosol Formation from Cyclohexene Ozonolysis: Effect of OH
780 Scavenger and the Role of Radical Chemistry. *Environ. Sci. & Technol.* **2004**, 38, 3343-
781 3350.
- 782 48. Keywood, M.D.; Varutbangkul, V.; Bahreini, R.; Flagan, R.C.; Seinfeld, J.H. Secondary
783 Organic Aerosol Formation from the Ozonolysis of Cycloalkenes and Related
784 Compounds. *Environ. Sci. & Technol.*, **2004**, 38, 4157-4164.

Table 1. Numbers of vehicles and analytical composite samples in light-duty vehicle test categories.

Category	Model Year	Odometer (miles)	Number of Vehicles	Number of Composites ^{1,2}
1	1996 and newer	low mileage (< 50,000)	4	1
2	1993-95	low mileage (< 75,000)	4	1
3	1996 and newer	high mileage (> 100,000)	4	1
4	1990-92	lower mileage (< 100,000)	4	1
5	1993-95	higher mileage (> 125,000)	8	2
6	1990-92	> 125,000	9	3
7	1986-89	> 125,000	6	3
8	1981-85	> 125,000	6	3
9	1980 and earlier	> 125,000	6	3
10	Smoker	no model year or odometer criteria	6	6
11	LD Diesel	no model year or odometer criteria	2	2
			59	26

1. Media composites for Categories 1 through 4 and laboratory composites for all other categories.

2. Separate composite samples for Phase 1 plus 2 of the UDC from a cold and warm start (52 composites total).

Table 2. Numbers of vehicles and analytical composite samples in heavy-duty diesel truck test categories.

Category	Model Year	Gross Vehicle Weight (lbs)	Number of Vehicles	Number of Composites ¹
1	Pre-1990	8,501 to 14,000	1	1
2	1990-93	8,501 to 14,000	1	
3	1994-97	8,501 to 14,000	2	1
4	1998 and newer	8,501 to 14,000	3	
5	Pre-1990	14,001 to 33,000	1	1
6	1990-93	14,001 to 33,000	0	0
7	1994-97	14,001 to 33,000	3	2
8	1998 and newer	14,001 to 33,000	3	
9	Pre-1990	33,001 to 80,000	2	2
10	1990-93	33,001 to 80,000	3	1
11	1994-97	33,001 to 80,000	7	3
12	1998 and newer	33,001 to 80,000	4	1
13	Bus		2	2
			32	14

1. Separate composite samples for CSHVR and HW cycles (28 composites total).

Table 3. Emission rates of OC, EC and sums of organic compounds by analytical composites and composite profile groupings.

Profile Composite ¹	Analytical Composite	IMPROVE				STN			Sum High MW PAH ² (mg/mile)	Sum of Hopanes (mg/mile)	Sum of Steranes (mg/mile)
		PM2.5 (mg/mile)	OC (mg/mile)	EC (mg/mile)	EC/TC	OC (mg/mile)	EC (mg/mile)	EC/TC			
<u>Light-Duty Gasoline</u>											
SI_LC	SI_1C1	8.0	3.9	1.2	0.23	4.0	0.6	0.14	0.0401	0.0013	0.0018
	SI_2C1	4.4	1.9	1.0	0.34	2.2	0.3	0.13	0.0148	0.0004	0.0029
	SI_6C2	7.5	6.0	2.3	0.28	5.8	1.6	0.22	0.0064	0.0011	0.0077
	SI_7C1	4.6	3.1	2.1	0.40	3.2	0.7	0.18	0.0055	0.0000	0.0067
SI_LW	SI_1W1	3.7	1.5	1.0	0.40	1.8	0.6	0.25	0.0164	0.0000	0.0021
	SI_2W1	1.9	1.2	0.4	0.23	1.5	0.0	0.02	0.0110	0.0000	0.0014
	SI_6W2	3.9	3.5	0.6	0.16	1.6	0.0	0.01	0.0017	0.0018	0.0089
	SI_7W1	2.1	2.1	1.3	0.37	2.5	0.7	0.20	0.0016	0.0000	0.0161
SI_HC	SI_10C2	52.8	46.3	6.6	0.13	40.0	9.2	0.19	0.0681	0.0935	0.0553
	SI_10C3	59.1	45.3	14.4	0.24	49.5	4.6	0.08	0.0609	0.0401	0.0874
	SI_5C1	13.1	4.5	1.2	0.21	5.0	0.2	0.03	0.0133	0.0000	0.0023
	SI_7C2	32.2	24.5	2.4	0.09	23.3	2.1	0.08	0.0095	0.1369	0.0422
	SI_7C3	31.9	26.5	2.0	0.07	23.6	1.1	0.04	0.0034	0.0270	0.0327
	SI_8C1	12.9	9.3	2.5	0.21	8.6	2.0	0.19	0.0106	0.0202	0.0112
	SI_10C1	13.3	12.5	3.3	0.21	13.3	2.6	0.16	0.0422	0.0933	0.0230
SI_HW	SI_10W1	17.8	16.1	1.2	0.07	15.3	0.8	0.05	0.0047	0.0953	0.0429
	SI_10W2	40.2	35.6	3.1	0.08	35.3	1.7	0.05	0.0138	0.0504	0.0310
	SI_10W3	10.1	13.6	4.5	0.25	12.7	2.7	0.18	0.0181	0.0038	0.0099
	SI_5W1	6.7	2.4	1.0	0.30	3.1	0.1	0.02	0.0046	0.0000	0.0029
	SI_7W2	15.8	11.6	2.0	0.15	11.3	1.9	0.14	0.0107	0.0800	0.0167
	SI_7W3	39.3	34.0	1.5	0.04	30.7	0.6	0.02	0.0008	0.0350	0.0355
	SI_8W1	6.7	7.0	1.5	0.18	6.2	0.8	0.11	0.0030	0.0311	0.0387
SI_BC	SI_4C1	6.2	1.7	1.8	0.51	2.1	1.2	0.37	0.0132	0.0001	0.0011
	SI_6C3	16.1	7.7	8.4	0.52	7.1	8.5	0.55	0.0357	0.0130	0.0068
	SI_8C2	26.4	11.9	13.9	0.54	11.2	13.8	0.55	0.0364	0.0482	0.0102
	SI_9C2	17.6	5.7	10.9	0.65	6.8	10.1	0.60	0.0386	0.0000	0.0071
SI_BW	SI_4W1	3.4	0.8	0.9	0.52	1.1	0.6	0.34	0.0058	0.0001	0.0011
	SI_6W3	5.9	4.3	3.2	0.43	3.4	3.1	0.48	0.0048	0.0021	0.0069
	SI_8W2	10.4	4.7	5.8	0.55	4.6	5.6	0.55	0.0166	0.0197	0.0073
	SI_9W2	6.4	2.2	3.5	0.62	2.9	2.6	0.47	0.0728	0.0260	0.0044
<u>Heavy-Duty Diesel</u>											
MDD	HW-5	1630.1	488.7	1332.4	0.73	454.6	1310.9	0.74	0.0000	0.1243	0.2186
MDD	HW-II	130.6	154.7	100.8	0.39	142.6	82.3	0.37	0.0000	0.0000	0.0000
MDD	HCS-5	1827.3	602.5	1490.2	0.71	575.1	1358.1	0.70	0.0025	0.2761	0.2940
MDD	HCS-IIb	445.7	363.0	247.9	0.41	330.2	198.1	0.38	0.0000	0.0000	0.2583
HDD; HW	HW-10	411.0	300.3	371.3	0.55	271.2	316.8	0.54	0.0000	0.1055	0.2714
HDD; HW	HW-11n	208.4	54.0	81.0	0.60	61.5	72.3	0.54	0.0002	0.0063	0.0148
HDD; HCS	HCS-10	1185.9	536.6	929.8	0.63	501.0	818.0	0.62	0.0000	0.3833	0.2239
HDD; HCS	HCS-11n	343.4	120.2	304.8	0.72	123.8	274.9	0.69	0.0007	0.0149	0.0322

1. Abbreviation for SI composites - H = High, L = Low, B = high black carbon; for CI composites - 1 = LHDT & MHDT, 2 = HHDT.

2. Sum of potential marker compounds for SI vehicle exhaust, benzo(ghi)perylene, indeno(1,2,3-cd)pyrene and coronene.

Table 4. Contributions of heavy molecular weight PAHs from the lubrication oil to the vehicle exhaust.

Analytical Composite	Lube Oil (ug/g)				Emission (ug/mile)		Emissions (g/mile)	% PAH from Lub Oil		OC/TC %
	Sum Hopanes	Sum Steranes	Sum 8 PAH	Sum 3 PAH	Sum 8 PAH	Sum 3 PAH	Oil	Sum 8 PAH	Sum 3 PAH	
SI_1C1	391.9	519.2	26.1	9.6	50.4	41.2	0.003	0.2%	0.1%	77.1%
SI_2C1	171.8	296.2	85.3	19.1	17.6	15.3	0.010	4.7%	1.2%	66.3%
SI_4C1	551.2	767.5	134.1	22.6	18.5	13.6	0.001	1.0%	0.2%	49.0%
SI_5C1	1377.4	1247.2	94.1	26.1	15.6	13.8	0.002	1.1%	0.3%	78.6%
SI_6C2	169.2	182.7	49.8	12.2	10.2	6.5	0.042	20.6%	7.9%	72.5%
SI_6C3	474.5	367.0	140.1	22.8	61.5	36.7	0.019	4.2%	1.2%	47.9%
SI_7C1	224.9	367.2	65.7	21.4	8.2	5.8	0.018	14.6%	6.7%	60.3%
SI_7C2	224.9	629.3	136.2	13.2	23.4	9.8	0.067	39.0%	9.0%	91.1%
SI_7C3	317.8	340.5	50.1	20.1	6.1	3.5	0.096	78.8%	55.0%	92.9%
SI_8C1	381.0	545.9	49.0	16.2	23.6	10.9	0.021	4.3%	3.1%	78.9%
SI_8C2	100.4	189.2	31.3	4.2	71	37.5	0.054	2.4%	0.6%	46.1%
SI_9C2	2769.8	2496.1	76.4	10.9	51.8	39.7	0.003	0.4%	0.1%	34.5%
SI_10C1	2192.9	1791.3	71.5	16.7	48.7	43.4	0.013	1.9%	0.5%	79.0%
SI_10C2	779.9	729.9	155.7	23.5	96.1	70.1	0.076	12.3%	2.5%	87.5%
SI_10C3	111.3	244.3	29.2	8.8	92.3	62.6	0.358	11.3%	5.1%	75.8%

Figure Captions

Figure 1. Emission rates (mg/mile) of zinc, calcium and phosphorus for (a) light-duty SI vehicles and (b) heavy-duty CI vehicles.

Figure 2. Distributions of emission rates by carbon fractions measured by TOR-IMPROVE method.

Figure 3. Ratios of elemental carbon measured by STN to IMPROVE as a function of EC concentrations and scatterplots of STN versus IMPROVE EC measurements for SI and CI exhaust samples.

Figure 4. Scatterplots of STN versus IMPROVE EC measurements for all CI and SI exhaust samples (upper panel) and for lower sample loadings (lower panel).

Figure 5. Variations in black carbon emissions during the UDC test cycle for very clean, normal and visibly smoking SI vehicle, and a light-duty diesel vehicle.

Figure 6. Emission rates of particulate polycyclic aromatic compounds. Species mnemonics are explained in Table S3.

Figure 7. Concentrations of particulate polycyclic aromatic compounds in diesel fuels and CI and SI vehicle lubrication oils.

Figure 8. Emission rates of hopanes and steranes. This result is inconsistent with previous studies that have shown similar composition of hopanes and steranes in SI and CI exhaust. Some CI samples were not included in the composite profile due to higher uncertainty caused by higher dilution ratios used in sample collection or invalid analytical results for other species.

Figure 9. Concentrations of steranes (upper panel) and hopanes (lower panel) in CI and SI vehicle lubrication oils.

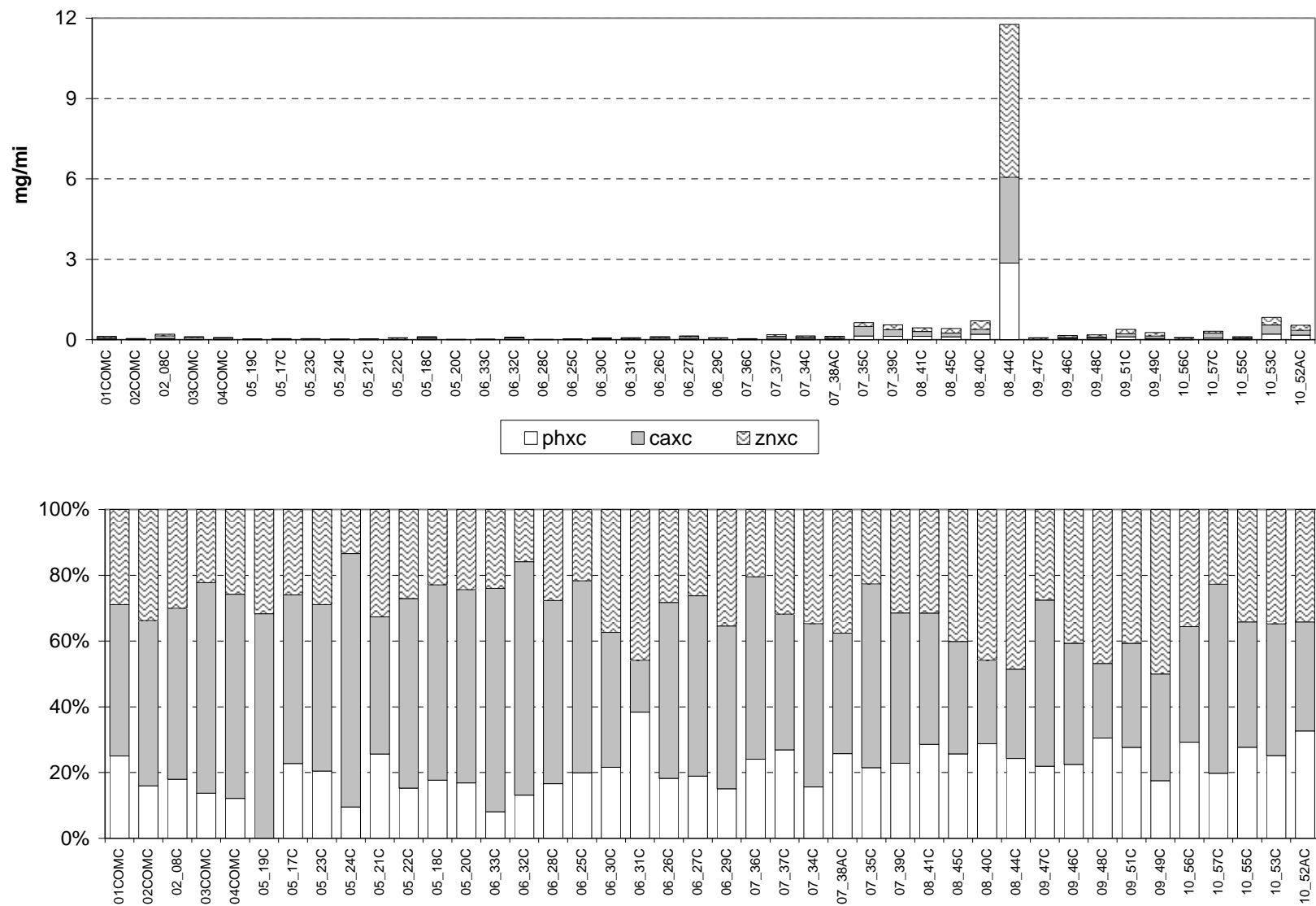


Figure 1a

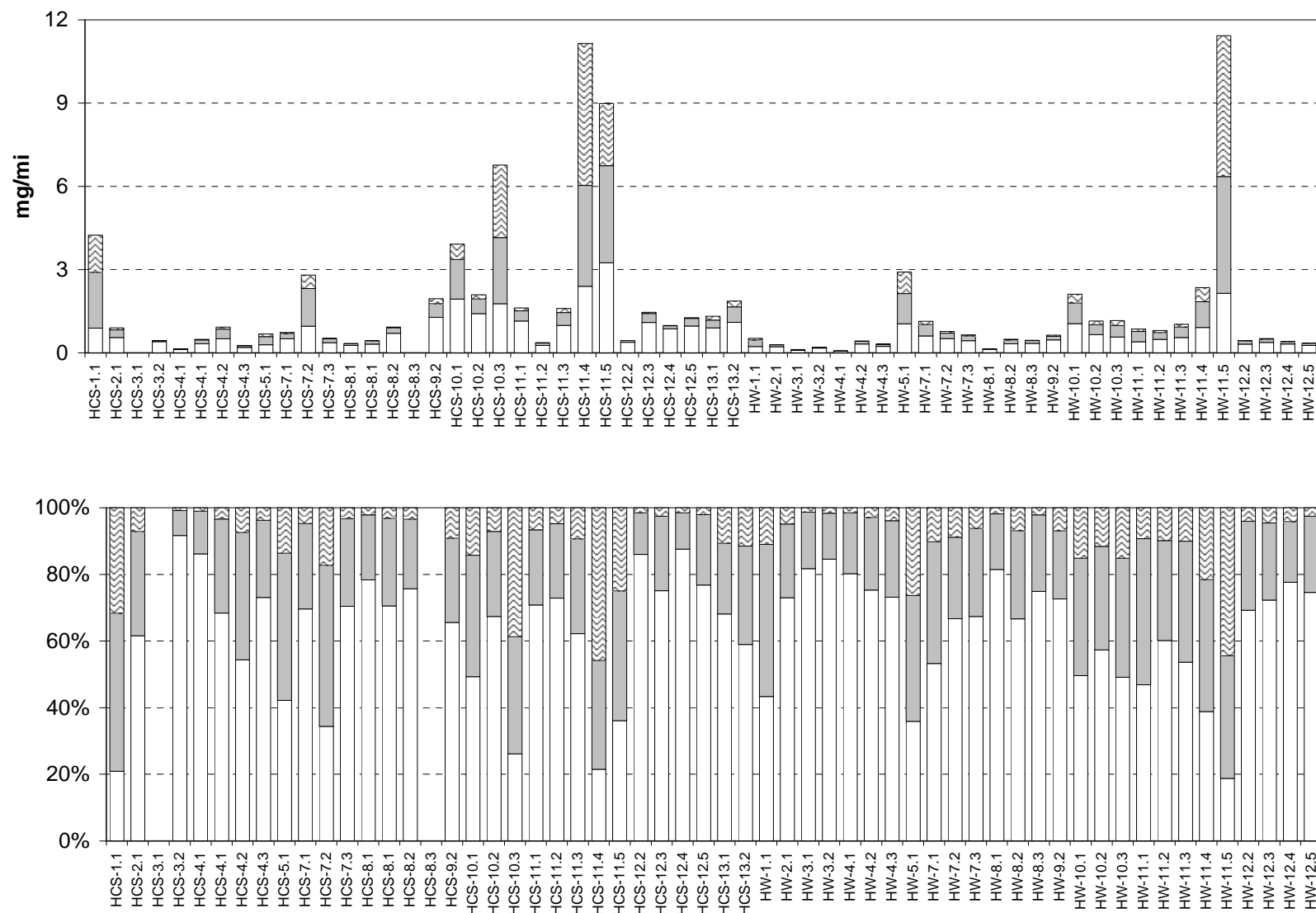


Figure 1b

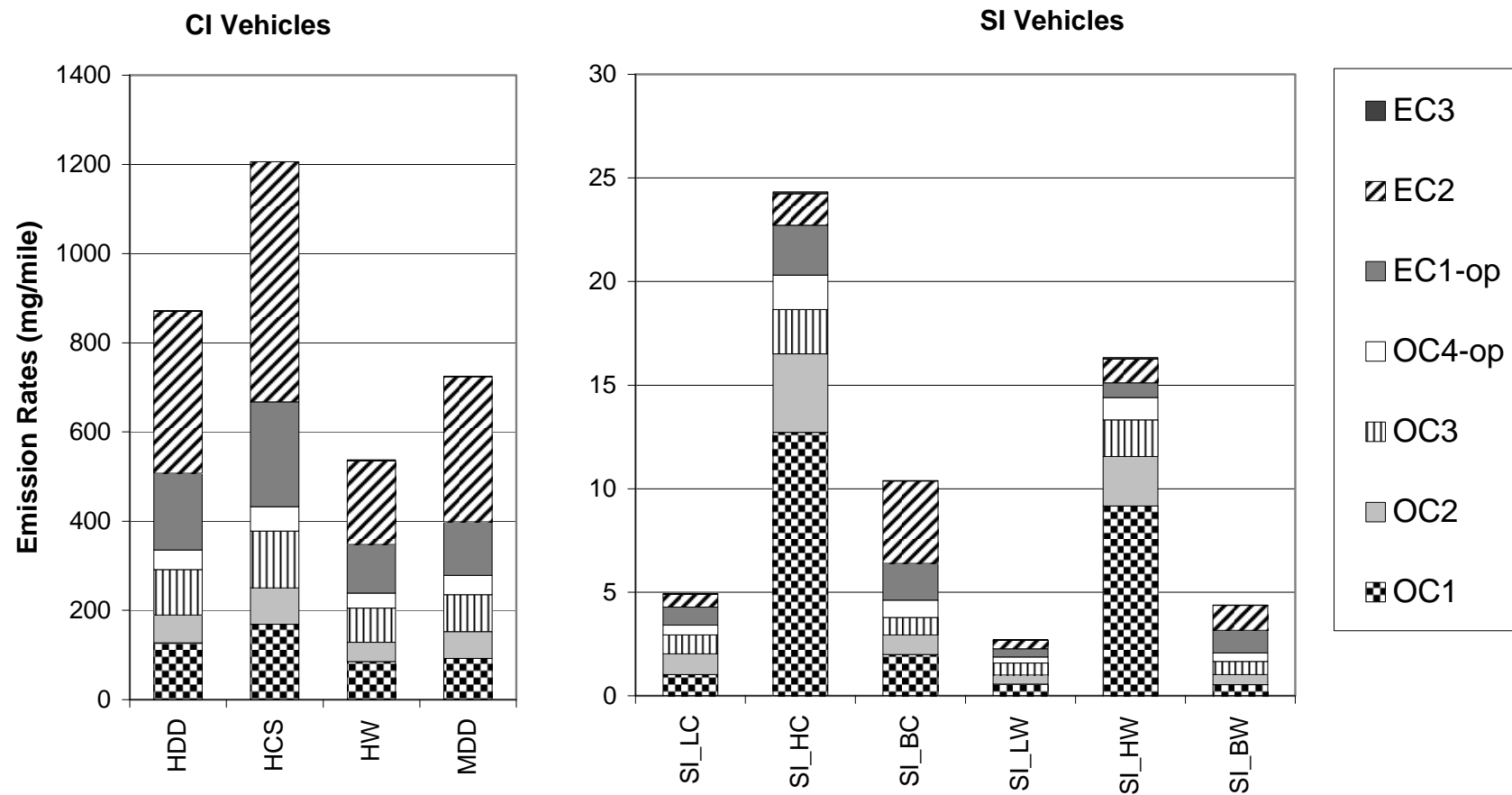


Figure 2

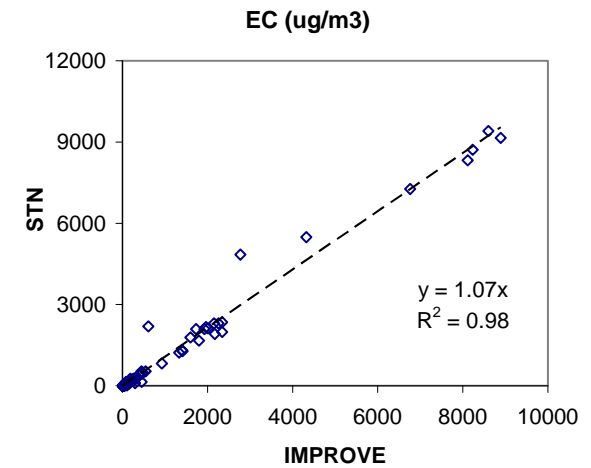
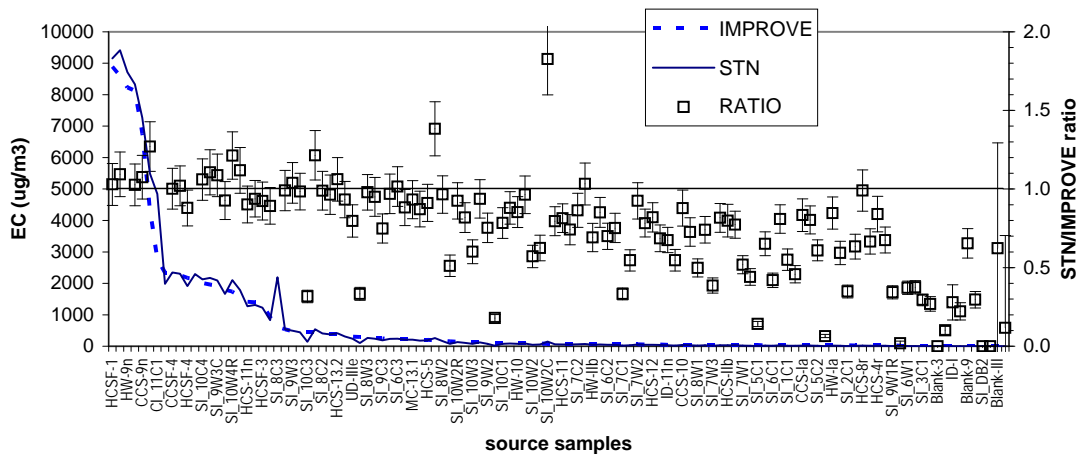
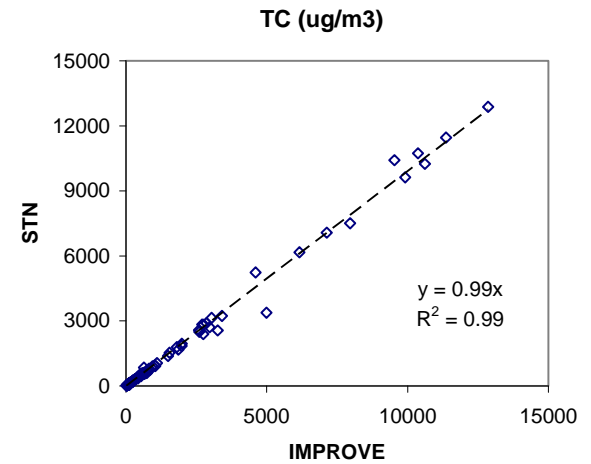
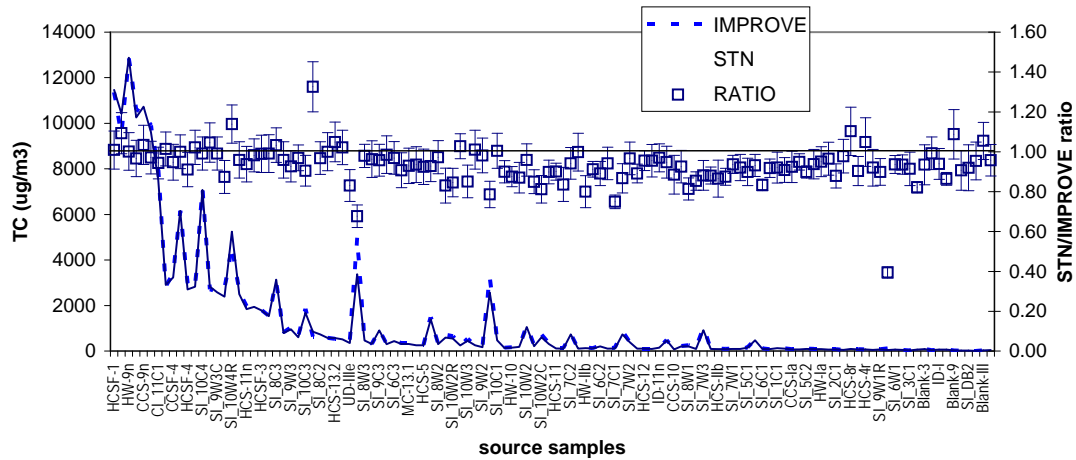


Figure 3.

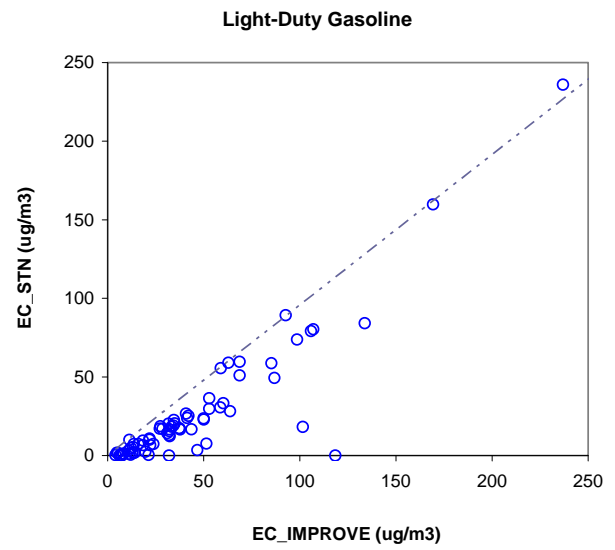
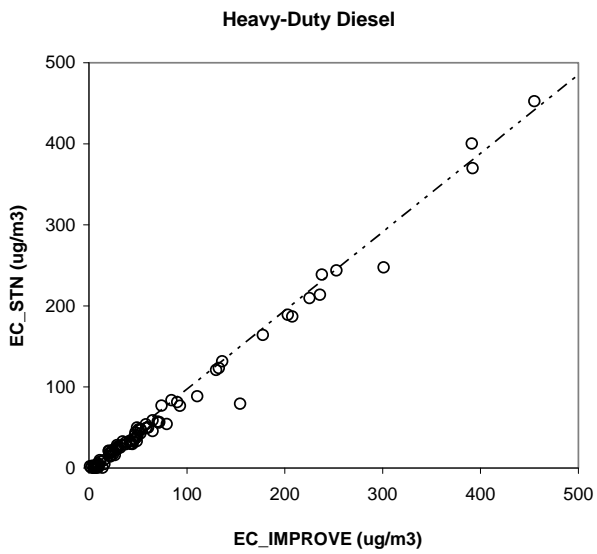
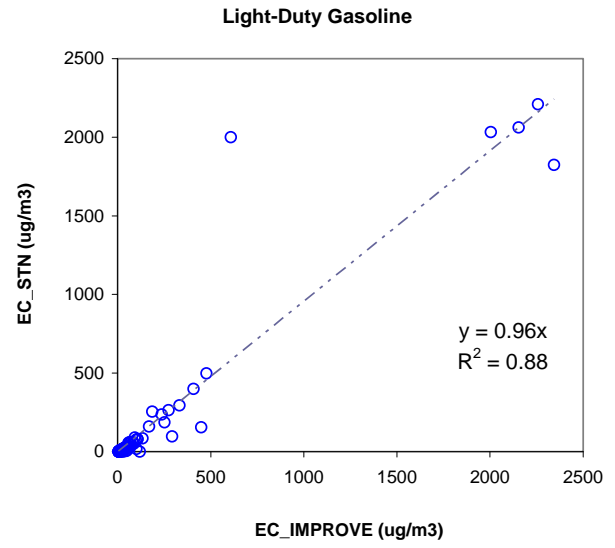
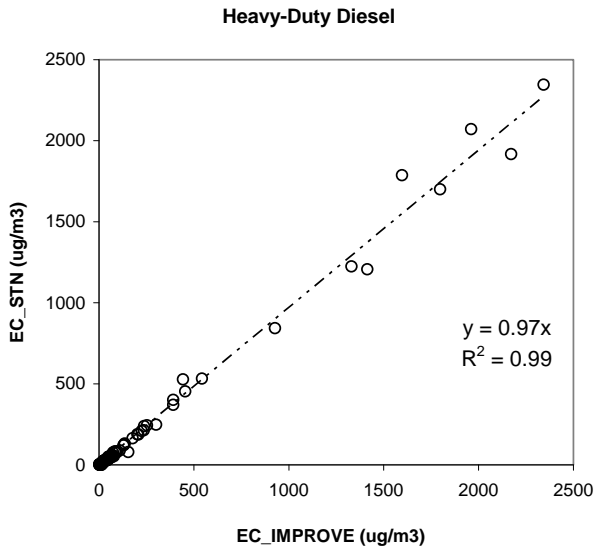


Figure 4

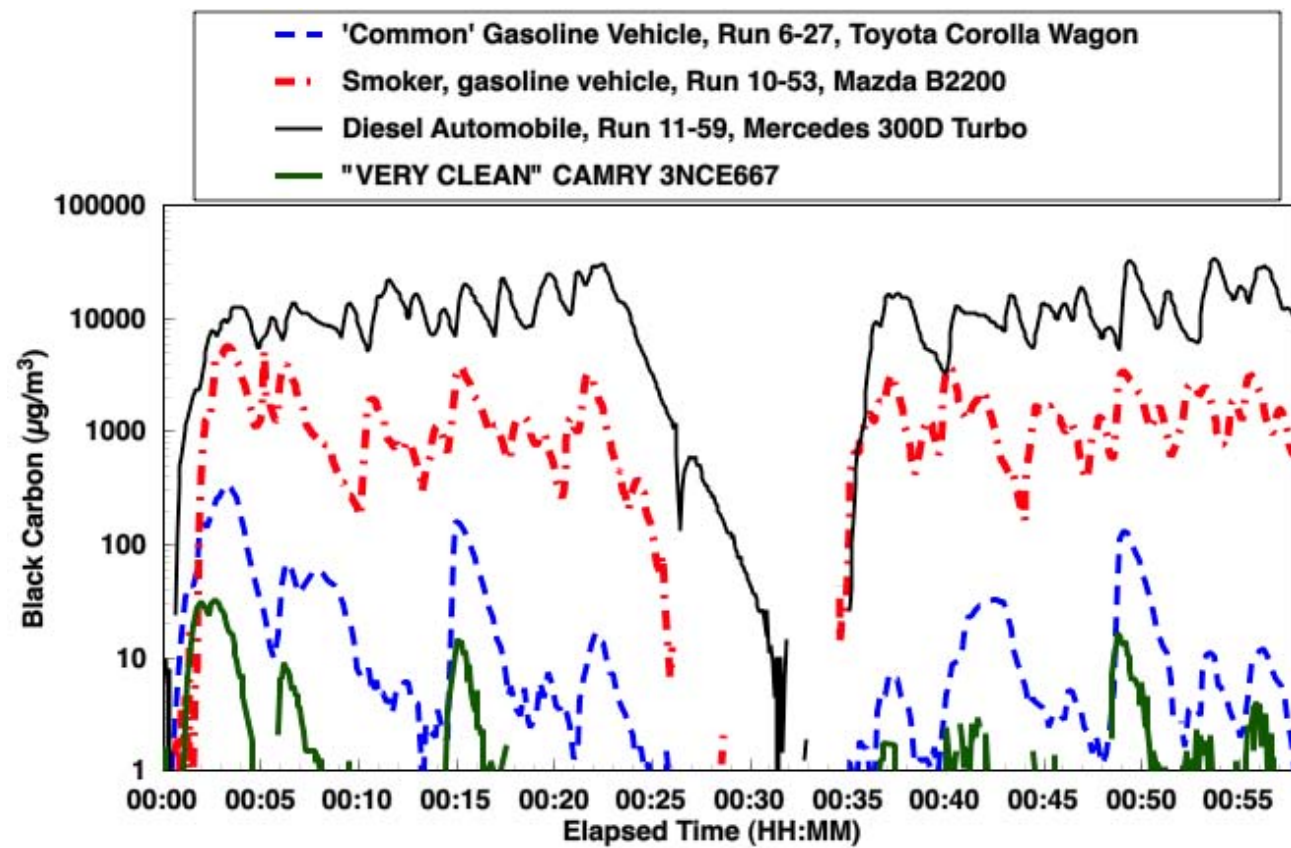


Figure 5.

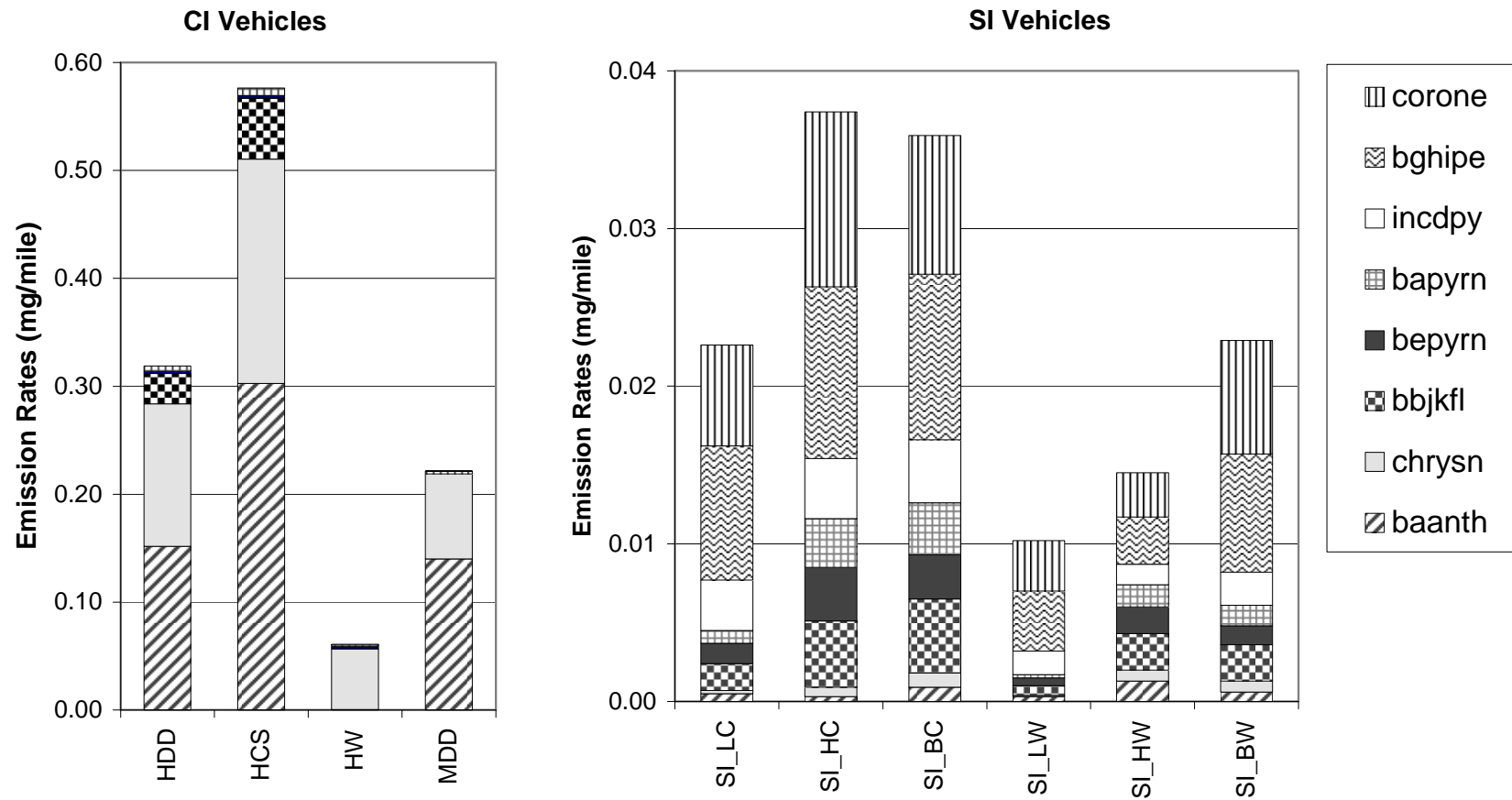


Figure 6

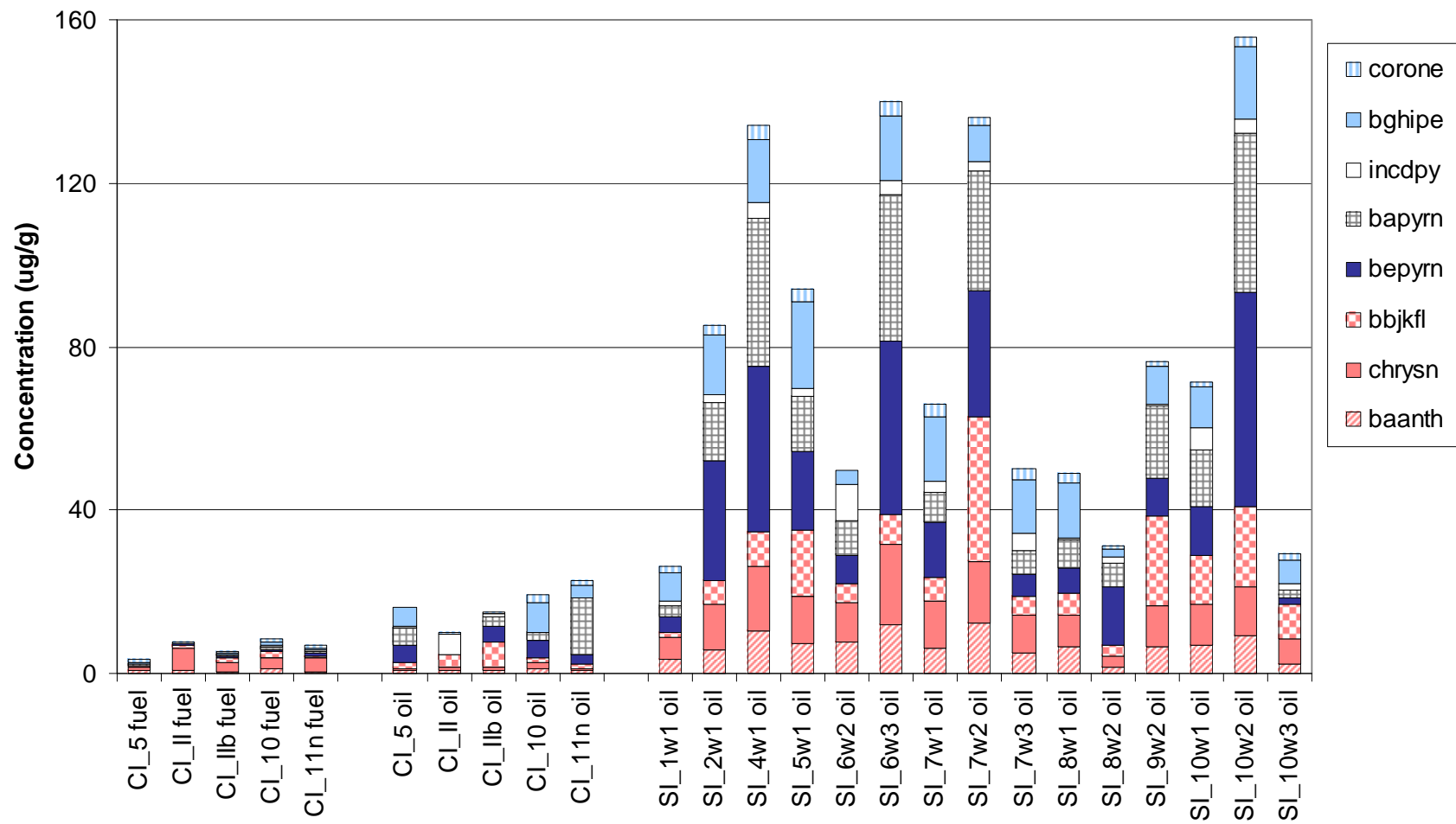


Figure 7

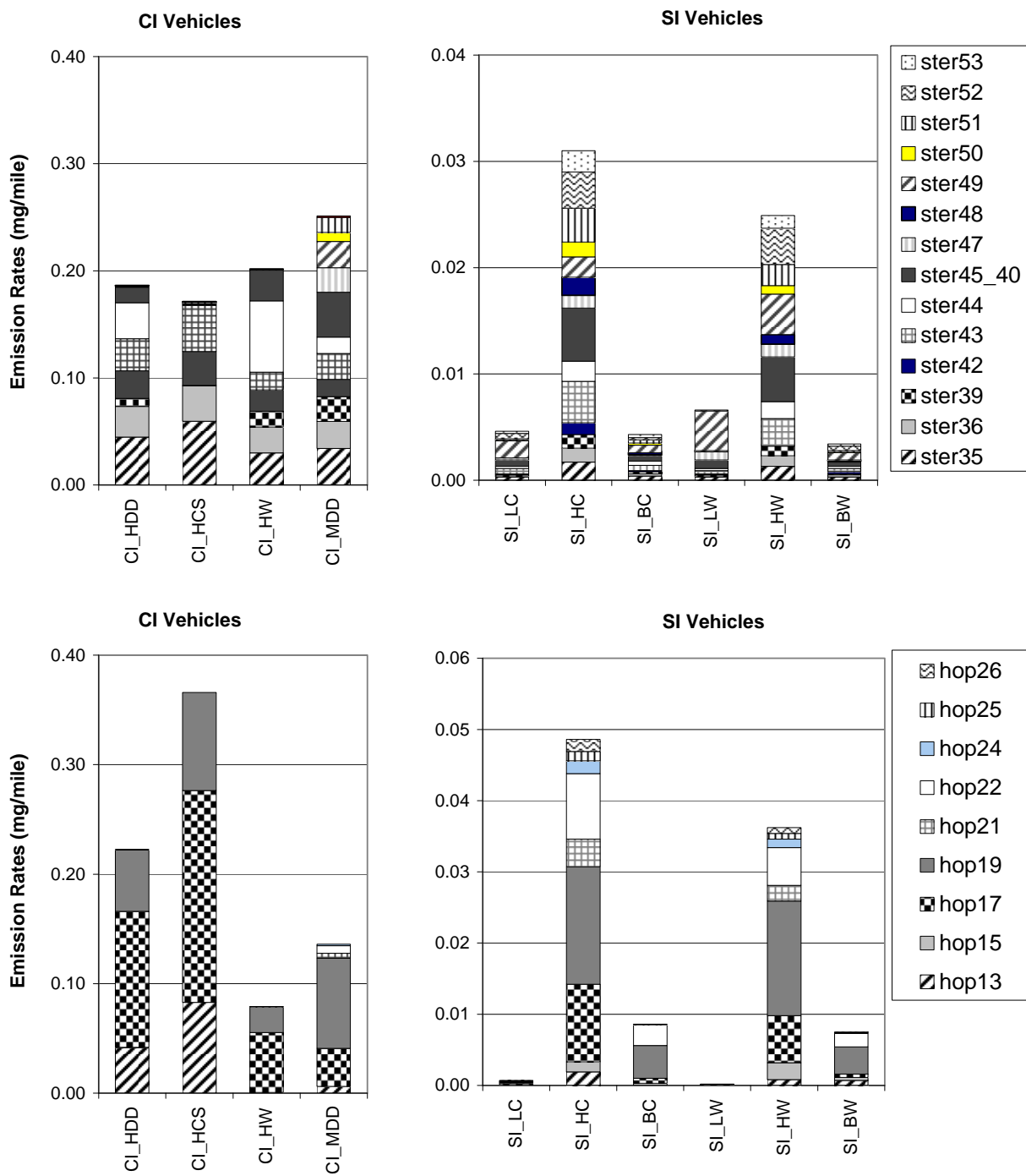


Figure 8

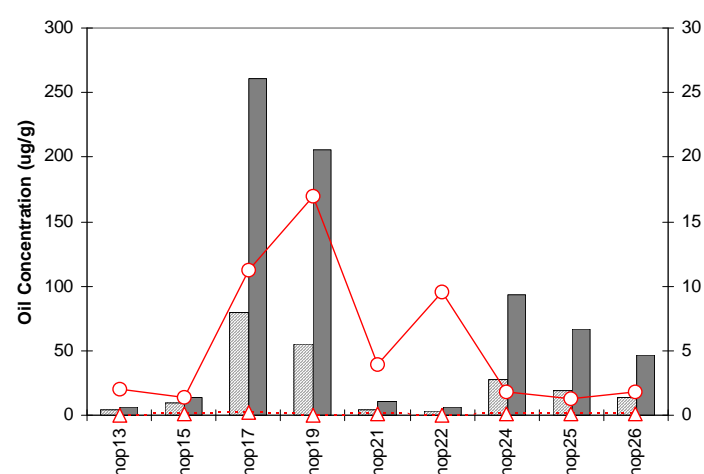
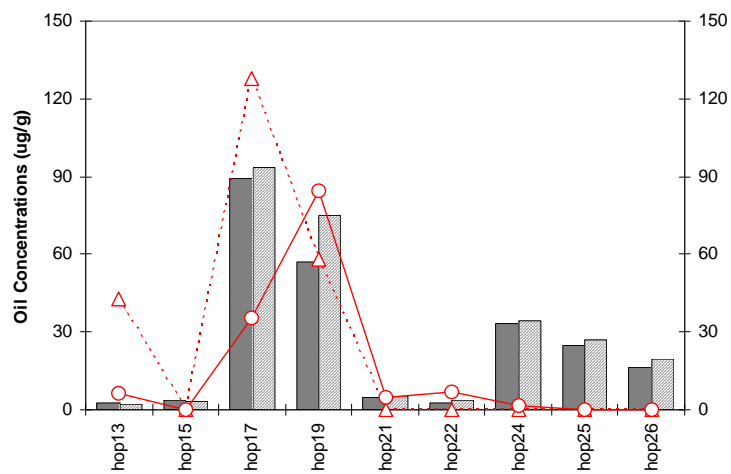
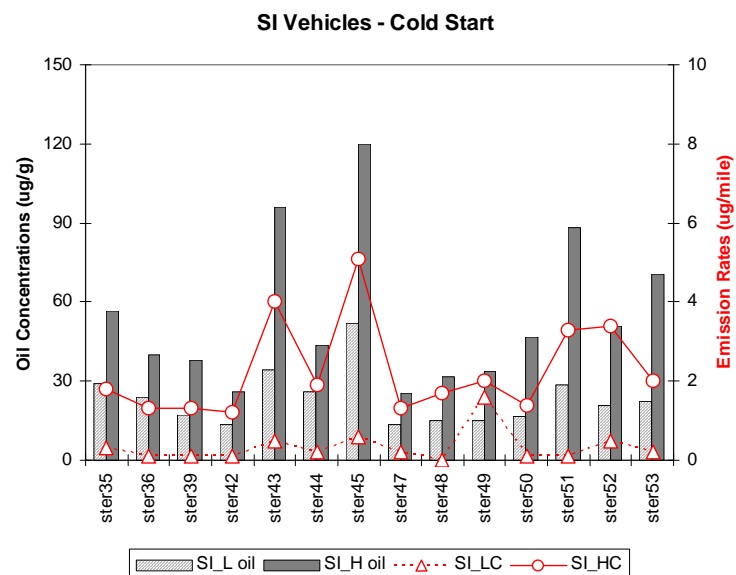
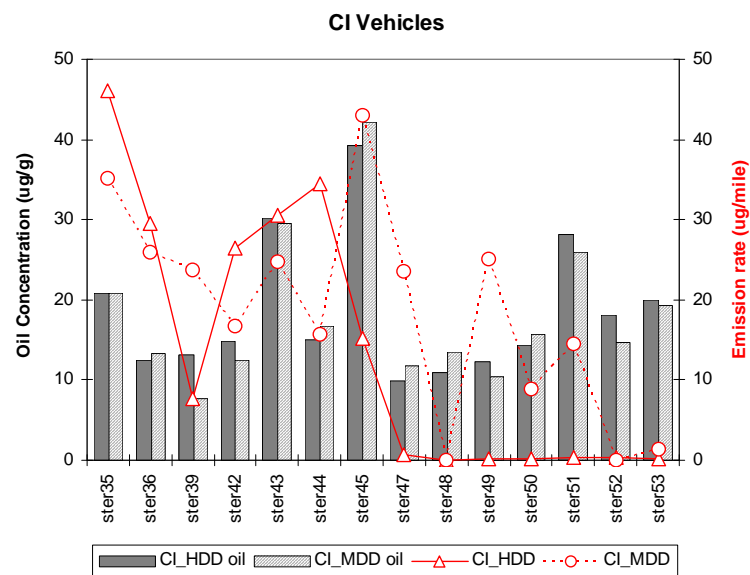


Figure 9

Supporting Information

Table S1. PM emission rates of light-duty vehicles and analytical compositing scheme for composition profiles.

Vehicle ID	Model Year	Make & Model	Odometer (miles)	UDC P1+P2 Cold Start		UDC P1+P2 Warm Start	
				Analytical Composite	PM _{2.5} (mg/mile)	Analytical Composite	PM _{2.5} (mg/mile)
1-1	1995	Toyota Camry	47502	SI_1C1*	8.0	SI_1W1*	3.7
1-2	1996	Dodge Dakota Sport	23283				
1-3	1995	GMC Yukon	59493				
1-4	1997	Jeep Cherokee Laredo	45359				
2-5	1995	Ford Explorer	32610	SI_2C1*	6.3	SI_2W1*	3.5
2-6	1995	Toyota Camry	45091				
2-7	1995	Ford Contour	33958				
2-8	1995	Pontiac Trans Sport	83413	SI_2C1	2.3	SI_2W1	0.4
3-9	1999	Ford Ranger XLT	121093	SI_3C1* (a)	1.6	SI_3W1* (a)	0.7
3-10	1996	Geo Prizm	125462				
3-11	1995	Toyota Camry	95350				
3-12	1995	Nissan Maxima	97329				
4-13	1991	Jeep Cherokee Laredo	83210	SI_4C1*	6.2	SI_4W1*	3.4
4-14	1992	BMW 3 Series	52773				
4-15	1992	Toyota Previa	134133				
4-16	1991	Mazda MX-6	70189				
5-17	1995	Ford Windstar	84744	SI_5C1	2.7	SI_5W1	2.1
5-18	1993	Geo Prizm	145260	SI_5C2	3.2	SI_5W2 (a)	1.3
5-19	1984	VW Vanagon	154225	SI_5C1	23.1	SI_5W1	11.0
5-20	1992	Ford Explorer	128,987	SI_5C2	3.5	SI_5W2 (a)	1.6
5-21	1993	Chevrolet Astro	140075	SI_5C2	6.3	SI_5W2 (a)	1.1
5-22	1994	Nissan Sentra	137702	SI_5C2	2.2	SI_5W2 (a)	0.9
5-23	1995	Dodge Caravan	103586	SI_5C2 (a)	1.0	SI_5W2 (a)	0.0
5-24	1994	Toyota Camry	216776	SI_5C2 (a)	0.9	SI_5W2 (a)	0.2
6-25	1992	Infiniti G20	137675	SI_6C1	2.4	SI_6W1 (a)	0.3
6-26	1991	Toyota Corolla	160012	SI_6C2	3.5	SI_6W2	2.1
6-27	1990	Toyota Corolla	149636	SI_6C2	11.4	SI_6W2	5.8
6-28	1992	Honda Accord	124080	SI_6C1	3.3	SI_6W1 (a)	0.6
6-29	1992	Dodge Caravan	160601	SI_6C3	16.1	SI_6W3	5.9
6-30	1991	Pontiac Trans Sport	120102	SI_6C1	5.8	SI_6W1 (a)	2.1
6-31	1991	Buick LeSabre	140958	SI_6C1 (a)	1.6	SI_6W1 (a)	0.3
6-32	1992	Honda Accord	172246	SI_6C1 (a)	1.4	SI_6W1 (a)	0.0
6-33	1995	Ford Explorer	120854	SI_6C1 (a)	1.7	SI_6W1 (a)	0.8
7-34	1988	Ford Ranger	92387	SI_7C1	5.2	SI_7W1	2.1
7-35	1987	Mazda Rx7	162367	SI_7C2	32.2	SI_7W2	15.8
7-36	1986	Chevrolet S-10	418371	SI_7C1	3.6	SI_7W1	1.8
7-37	1989	Plymouth Reliant	147518	SI_7C1	2.3	SI_7W1	2.5
7-38A	1987	Olds Cutlass	118459	SI_7C1	7.2	SI_7W1	1.8
7-39	1989	Acura Legend	174142	SI_7C3	31.9	SI_7W3	39.3
8-40	1985	Toyota Tacoma	212037	SI_8C2	26.4	SI_8W2	10.4
8-41	1984	Toyota Corolla	248202	SI_8C1	18.9	SI_8W1	10.3
8-42	1982	Chevrolet Silverado 20	148210				
8-43	1981	Chrysler Imperial	151948				
8-44	1984	Toyota Pickup	167579	SI_8C3	139.7	SI_8W3	13.7
8-45	1983	Toyota Celica	197122	SI_8C1	7.0	SI_8W1	3.1
8-46	1979	Mercedes 450 Sl	159085	SI_9C1	5.3	SI_9W1	4.2
8-47	1980	Honda Accord	182190	SI_9C1 (a)	1.7	SI_9W1 (a)	0.8
9-48	1977	Chevrolet Luv	158928	SI_9C2	17.6	SI_9W2	6.4
9-49	1980	Toyota Celica	98349	SI_9C4	94.0	SI_9W4	111.4
9-50	1979	Toyota Corolla	121813	SI_9C3	37.7	SI_9W3	35.8
10-52A	1969	Chevrolet Chevelle Malibu	147674	SI_10C5 (b)	219.2	SI_10W5	127.2
10-53	1988	Mazda B2200 PU	149811	SI_10C4 (b)	251.9	SI_10W4 (b)	207.9
10-54	1989	Mitsubishi Mighty Max	273290				
10-55	1978	Chevrolet Caprice Classic	128913	SI_10C3	59.1	SI_10W3	10.1
10-56	1989	Toyota Tacoma	421092	SI_10C1	13.3	SI_10W1	17.8
10-57	1990	Vw Jetta	259488	SI_10C2	52.8	SI_10W2	40.2
11-58	1982	Chevrolet 1500 High Sierra	162308	CI_11C1	305.2	CI_11W1	295.2
11-59	1983	Mercedes 300D	361112				

* Same sampling media used for test within vehicle category ("media composites").

(a) Sample loading too low for valid organic speciation.

(b) Sample loading too high for reliable carbon analysis

Table S2. PM emission rates of heavy-duty diesel vehicles and analytical compositing scheme for composition profiles.

Vehicle ID	Model Year	Manufacturer	Type	GVW (lbs)	Odometer (miles)	Hot CSR PM (mg/mi)		Highway PM (mg/mi)	
						Analytical Composite	PM _{2.5} (mg/mile)	Analytical Composite	PM _{2.5} (mg/mile)
1.1	1989	Ford	Box Truck	11000	55973	HCS-Ia (a)	358	HW-Ia (a)	106
2.1	1990	Ford	Tractor Truck	11000		HCS-Ia (a)	122	HW-Ia (a)	66
3.1	1997	Isuzu	Box Truck	12000	114493	HCS-Ib (a)	159	HW-Ib (a)	65
3.2	1997	GMC	Box Truck	10000	86944	HCS-Ib (a)	231	HW-Ib (a)	74
4.1	2000	Isuzu	Box Truck	12000	45164	HCS-Ib (a)	153	HW-Ib (a)	87
4.2	2000	Ford	Van	9500	27965	HCS-Ib (a)	176	HW-Ib (a)	86
4.3	2000	Isuzu	Box Truck	14000	361	HCS-Ib (a)	148	HW-Ib (a)	90
5.1	1988	Ford	Box Truck	26500	170556	HCS-5		HW-5	
5.2	1988	International	Box Truck	18000	169008				
7.1	1995	GM	Box Truck	25950	92000	HCS-II (a)	99	HW-II	205
7.2	1995	International	Flat Bed	25500	151601	HCS-IIb	445	HW-IIb (a)	155
7.3	1996	Freightliner	Box Truck	26000	162300	HCS-II	70	HW-II	67
8.1	1999	Isuzu	Box Truck	19500	15840	HCS-II	153	HW-II	59
8.2	1999	International	Box Truck	25500	56835	HCS-II	340	HW-II	207
8.3	1999	Freightliner	Box Truck	26000	49251	HCS-II		HW-II	119
9.1	1985	International	Tractor Truck	32000	501586	HCS-9n		HW-9n	
9.2	1985	Freightliner	Tractor Truck	80000	36252	HCS-9e		HW-9e	
10.1	1992	Ford	Tractor Truck	48000	769413	HCS-10	862	HW-10	440
10.2	1993	Freightliner	Tractor Truck	52000	842140	HCS-10	680	HW-10	414
10.3	1992	Volvo	Tractor Truck	46000	109897	HCS-10		HW-10	369
11.1	1994	Freightliner	Tractor Truck	52000	109897	HCS-11	539	HW-11	206
11.2	1994	Freightliner	Tractor Truck	80000	602338	HCS-11	392	HW-11	239
11.3	1997	Ford	Tractor Truck	46000	449600	HCS-11	505	HW-11	166
11.4	1997	Volvo	Tractor Truck	50000	437500	HCS-11	1041	HW-11	420
11.5	1996	Volvo	Tractor Truck	50350	472927	HCS-11	1125	HW-11	520
11.6	1994	Freightliner	Tractor Truck	52000		HCS-11n	343	HW-11n	208
11.7	1995	Freightliner	Tractor Truck	50000	241843	HCS-11e	493	HW-11e (a)	8
12.2	1999	Sterling	Tractor Truck	52000	272307	HCS-12	523	HW-12	225
12.3	2000	Sterling	Tractor Truck	52000	255880	HCS-12	412	HW-12	143
12.4	2001	Volvo	Tractor Truck	52000	145749	HCS-12	313	HW-12	185
12.5	1998	Sterling	Tractor Truck	52000	327300	HCS-12	417	HW-12	128
13.1	1992	TMC	Transit Bus	39500	519395	HCS-13.1 (a)	865		
13.2	1982	GMC	Transit Bus	36900	103143	HCS-13.2 (a)			

(a) Sample loading too low for valid organic speciation.

Table S3. Speciated Emission Rates for Composite Diesel and Gasoline Exhaust Profiles.

Species Description	Nmemonic	HDD	HCS	HW	MDD	SI_BC	SI_BW	SI_HC	SI_HW	SI_LC	SI_LW
<u>PM mass and IMPROVE carbon (mg/mile)</u>											
PM _{2.5} Mass	MSGC	667.8 ± 11.8	975.3 ± 22.2	360.4 ± 8.2	569.5 ± 17.3	12.1 ± 0.3	5.2 ± 0.1	26.8 ± 0.5	16.6 ± 0.4	5.9 ± 0.1	2.8 ± 0.0
Total Carbon (TC)	TC	871.8 ± 17.9	1206.1 ± 32.3	537.4 ± 15.3	725.3 ± 26.8	10.4 ± 0.5	4.4 ± 0.2	24.3 ± 2.1	16.3 ± 1.5	4.9 ± 0.1	2.7 ± 0.1
Organic Carbon (OC)	OCTC	335.6 ± 14.1	432.5 ± 24.7	238.7 ± 13.5	278.5 ± 19.1	4.6 ± 0.5	2.1 ± 0.2	20.3 ± 2.0	14.4 ± 1.5	3.4 ± 0.1	1.9 ± 0.1
Elemental Carbon (EC)	ECTC	536.1 ± 11.0	773.5 ± 20.9	298.7 ± 7.2	446.8 ± 18.9	5.8 ± 0.2	2.3 ± 0.1	4.0 ± 0.1	1.9 ± 0.0	1.5 ± 0.0	0.8 ± 0.0
OC Fraction 1	O1TC	127.1 ± 9.9	169.3 ± 17.6	85.0 ± 9.2	92.2 ± 13.6	2.0 ± 0.4	0.5 ± 0.1	12.7 ± 2.0	9.2 ± 1.4	1.0 ± 0.1	0.6 ± 0.1
OC Fraction 2	O2TC	62.6 ± 4.6	81.5 ± 8.1	43.7 ± 4.3	60.3 ± 6.7	1.0 ± 0.1	0.5 ± 0.1	3.8 ± 0.4	2.4 ± 0.3	1.0 ± 0.1	0.4 ± 0.0
OC Fraction 3	O3TC	101.9 ± 8.6	127.1 ± 14.9	76.8 ± 8.6	82.6 ± 11.3	0.8 ± 0.1	0.6 ± 0.1	2.1 ± 0.2	1.8 ± 0.2	0.9 ± 0.1	0.6 ± 0.0
OC Fraction 4 + Pyrolyzed OC O4_OP		44.0 ± 2.1	54.7 ± 3.7	33.3 ± 2.0	43.4 ± 2.7	0.8 ± 0.3	0.4 ± 0.0	1.7 ± 0.2	1.1 ± 0.2	0.5 ± 0.0	0.3 ± 0.0
EC Fraction 1 - Pyrolyzed EC E1_OP		172.0 ± 27.5	235.0 ± 50.3	108.9 ± 22.4	120.5 ± 32.6	1.8 ± 0.4	1.1 ± 0.1	2.4 ± 0.3	0.7 ± 0.3	0.9 ± 0.0	0.4 ± 0.0
EC Fraction 2	E2TC	363.0 ± 13.5	538.1 ± 25.4	187.9 ± 9.3	325.1 ± 26.6	4.0 ± 0.4	1.2 ± 0.1	1.5 ± 0.1	1.1 ± 0.1	0.6 ± 0.0	0.4 ± 0.0
EC Fraction 3	E3TC	1.1 ± 0.3	0.3 ± 0.4	1.9 ± 0.3	1.2 ± 0.3	0.0 ± 0.0	0.0 ± 0.0	0.1 ± 0.0	0.1 ± 0.0	0.0 ± 0.0	0.0 ± 0.0
<u>STN carbpm (mg/mile)</u>											
NIOSH OC	OC_STN	312.7 ± 11.9	406.7 ± 21.5	218.7 ± 10.0	259.1 ± 12.7	4.8 ± 0.2	2.2 ± 0.1	19.7 ± 0.5	13.8 ± 0.4	3.5 ± 0.1	1.9 ± 0.0
NIOSH EC	EC_STN	469.0 ± 13.7	682.2 ± 25.8	255.7 ± 9.3	409.8 ± 20.1	5.3 ± 0.2	2.0 ± 0.1	2.6 ± 0.2	1.0 ± 0.2	0.7 ± 0.0	0.4 ± 0.0
<u>Elements (mg/mile)</u>											
Chloride	CLIC	2.11 ± 0.53	3.74 ± 0.98	0.48 ± 0.40	1.16 ± 0.53	0.04 ± 0.00	0.02 ± 0.00	0.07 ± 0.01	0.07 ± 0.01	0.04 ± 0.00	0.02 ± 0.00
Nitrate	N3IC	0.12 ± 0.49	0.00 ± 0.90	0.25 ± 0.39	3.41 ± 0.62	0.11 ± 0.01	0.08 ± 0.01	0.08 ± 0.01	0.08 ± 0.01	0.10 ± 0.00	0.08 ± 0.00
Sulfate	S4IC	11.33 ± 0.54	14.90 ± 0.97	7.77 ± 0.46	16.44 ± 0.62	0.59 ± 0.02	0.20 ± 0.01	0.54 ± 0.02	0.18 ± 0.01	0.54 ± 0.01	0.26 ± 0.01
Ammonium	N4CC	3.01 ± 0.50	3.75 ± 0.91	2.27 ± 0.41	6.05 ± 0.56	0.25 ± 0.01	0.10 ± 0.01	0.20 ± 0.01	0.07 ± 0.01	0.25 ± 0.01	0.12 ± 0.00
Soluble Potassium	KPAC	1.04 ± 0.06	1.51 ± 0.12	0.56 ± 0.05	0.61 ± 0.07	0.00 ± 0.00	0.00 ± 0.00	0.01 ± 0.00	0.01 ± 0.00	0.00 ± 0.00	0.00 ± 0.00
Sodium (qualitative only)	NAXC	0.97 ± 0.46	0.68 ± 0.88	1.26 ± 0.23	1.54 ± 0.39	0.01 ± 0.01	0.00 ± 0.01	0.01 ± 0.01	0.01 ± 0.01	0.00 ± 0.00	0.01 ± 0.00
Magnesium (qualitative only)	MGXC	0.49 ± 0.27	0.83 ± 0.50	0.14 ± 0.20	0.66 ± 0.27	0.02 ± 0.00	0.01 ± 0.00	0.04 ± 0.00	0.04 ± 0.00	0.01 ± 0.00	0.01 ± 0.00
Aluminum	ALXC	0.99 ± 0.12	1.57 ± 0.19	0.41 ± 0.13	1.20 ± 0.09	0.01 ± 0.00	0.00 ± 0.00	0.01 ± 0.00	0.01 ± 0.00	0.01 ± 0.00	0.00 ± 0.00
Silicon	SIXC	8.24 ± 0.13	12.22 ± 0.25	4.26 ± 0.09	6.36 ± 0.19	0.41 ± 0.01	0.31 ± 0.01	0.56 ± 0.01	0.42 ± 0.01	0.21 ± 0.00	0.11 ± 0.00
Phosphorous	PHXC	1.05 ± 0.03	1.45 ± 0.06	0.66 ± 0.03	0.51 ± 0.09	0.03 ± 0.00	0.04 ± 0.00	0.08 ± 0.00	0.05 ± 0.00	0.02 ± 0.00	0.01 ± 0.00
Sulfur	SUXC	5.11 ± 0.08	6.94 ± 0.15	3.28 ± 0.07	7.12 ± 0.13	0.24 ± 0.01	0.08 ± 0.00	0.23 ± 0.01	0.10 ± 0.00	0.21 ± 0.00	0.10 ± 0.00
Chlorine	CLXC	0.49 ± 0.09	0.88 ± 0.15	0.11 ± 0.10	0.51 ± 0.10	0.03 ± 0.00	0.01 ± 0.00	0.03 ± 0.00	0.01 ± 0.00	0.03 ± 0.00	0.01 ± 0.00
Potassium	KPXC	0.70 ± 0.07	1.15 ± 0.11	0.25 ± 0.08	0.70 ± 0.07	0.00 ± 0.00	0.00 ± 0.00	0.01 ± 0.00	0.00 ± 0.00	0.00 ± 0.00	0.00 ± 0.00
Calcium	CAXC	4.41 ± 0.08	6.33 ± 0.14	2.49 ± 0.06	2.98 ± 0.09	0.04 ± 0.00	0.10 ± 0.00	0.15 ± 0.00	0.13 ± 0.00	0.04 ± 0.00	0.02 ± 0.00
Chromium	CRXC	0.03 ± 0.06	0.04 ± 0.12	0.01 ± 0.03	0.00 ± 0.06	0.00 ± 0.00	0.00 ± 0.00	0.00 ± 0.00	0.00 ± 0.00	0.00 ± 0.00	0.00 ± 0.00
Manganese	MNXC	0.01 ± 0.03	0.01 ± 0.06	0.01 ± 0.02	0.00 ± 0.04	0.00 ± 0.00	0.00 ± 0.00	0.00 ± 0.00	0.00 ± 0.00	0.00 ± 0.00	0.00 ± 0.00
Iron	FEXC	5.73 ± 0.10	9.88 ± 0.20	1.59 ± 0.03	3.57 ± 0.10	0.02 ± 0.00	0.02 ± 0.00	0.06 ± 0.00	0.03 ± 0.00	0.03 ± 0.00	0.02 ± 0.00
Nickel	NIXC	0.01 ± 0.02	0.02 ± 0.03	0.00 ± 0.01	0.00 ± 0.02	0.00 ± 0.00	0.00 ± 0.00	0.00 ± 0.00	0.00 ± 0.00	0.00 ± 0.00	0.00 ± 0.00
Copper	CUXC	0.15 ± 0.01	0.24 ± 0.01	0.06 ± 0.01	0.04 ± 0.02	0.00 ± 0.00	0.00 ± 0.00	0.02 ± 0.00	0.02 ± 0.00	0.00 ± 0.00	0.00 ± 0.00
Zinc	ZNXC	2.90 ± 0.04	4.43 ± 0.09	1.37 ± 0.02	1.10 ± 0.03	0.05 ± 0.00	0.04 ± 0.00	0.10 ± 0.00	0.07 ± 0.00	0.02 ± 0.00	0.01 ± 0.00
Bromine	BRXC	0.02 ± 0.02	0.03 ± 0.03	0.00 ± 0.02	0.24 ± 0.02	0.00 ± 0.00	0.00 ± 0.00	0.00 ± 0.00	0.00 ± 0.00	0.00 ± 0.00	0.00 ± 0.00
Rubidium	RBXC	0.00 ± 0.02	0.00 ± 0.03	0.00 ± 0.01	0.00 ± 0.02	0.00 ± 0.00	0.00 ± 0.00	0.00 ± 0.00	0.00 ± 0.00	0.00 ± 0.00	0.00 ± 0.00
Strontium	SRXC	0.02 ± 0.02	0.03 ± 0.03	0.01 ± 0.02	0.02 ± 0.02	0.00 ± 0.00	0.00 ± 0.00	0.00 ± 0.00	0.00 ± 0.00	0.00 ± 0.00	0.00 ± 0.00
Molybdenum	MOXC	0.03 ± 0.05	0.04 ± 0.09	0.01 ± 0.04	0.00 ± 0.06	0.00 ± 0.00	0.00 ± 0.00	0.00 ± 0.00	0.00 ± 0.00	0.00 ± 0.00	0.00 ± 0.00
Barium	BAXC	1.56 ± 1.14	2.84 ± 2.07	0.29 ± 0.93	0.87 ± 1.36	0.01 ± 0.01	0.01 ± 0.01	0.01 ± 0.02	0.03 ± 0.02	0.01 ± 0.00	0.01 ± 0.00
Lead	PBXC	0.10 ± 0.06	0.17 ± 0.11	0.03 ± 0.05	0.01 ± 0.07	0.00 ± 0.00	0.00 ± 0.00	0.01 ± 0.00	0.01 ± 0.00	0.00 ± 0.00	0.00 ± 0.00

Table S3 (continued). Speciated emission rates for composite diesel and gasoline exhaust profiles.

Species Description	Nmemonic	HDD	HCS	HW	MDD	SI_BC	SI_BW	SI_HC	SI_HW	SI_LC	SI_LW
<u>Polycyclic aromatic hydrocarbons (ug/mile)</u>											
Naphthalene	NAPHTH	21226 ± 678	42376 ± 1353	77 ± 73	8432 ± 215	3000 ± 72	515 ± 14	2520 ± 71	4732 ± 119	1390 ± 23	763 ± 17
Sum of methyl naphthalenes	MNAPH	2137 ± 41	3125 ± 77	1148 ± 28	1232 ± 38	1560 ± 32	301 ± 8	1735 ± 44	2800 ± 66	942 ± 14	377 ± 7
Biphenyl	BIPHEN	273 ± 10	440 ± 20	106 ± 6	58 ± 7	56 ± 1	12 ± 0	70 ± 2	140 ± 4	30 ± 1	15 ± 0
1+2ethylnaphthalene	ENAP12	734 ± 25	1179 ± 49	288 ± 14	654 ± 28	79 ± 2	17 ± 1	86 ± 3	138 ± 5	42 ± 1	13 ± 0
Sum of dimethyl naphthalenes	DMNAPH	1912 ± 86	2569 ± 149	1255 ± 88	1177 ± 104	309 ± 24	66 ± 10	343 ± 20	576 ± 27	138 ± 9	47 ± 6
Sum of methylbiphenyls	MBPH	18743 ± 446	35897 ± 878	1588 ± 158	821 ± 321	22 ± 15	2 ± 10	28 ± 13	69 ± 22	3 ± 9	1 ± 9
Bibenzyl	BIBENZ	0.0 ± 524.2	0.0 ± 643.9	0.0 ± 827.3	0.0 ± 746.6	105.1 ± 15.2	41.2 ± 8.5	33.2 ± 13.2	81.2 ± 18.6	30.9 ± 6.5	17.1 ± 6.8
Dibenzofuran	DBZFUR	141.5 ± 4.9	207.2 ± 9.2	75.8 ± 3.6	91.0 ± 5.2	18.9 ± 0.5	6.0 ± 0.2	22.8 ± 0.8	36.9 ± 1.2	10.7 ± 0.3	4.7 ± 0.1
Sum of trimethyl naphthalene	TMNAPH	975.1 ± 18.3	1414.2 ± 33.5	536.1 ± 14.9	762.4 ± 21.0	105.9 ± 1.4	19.3 ± 0.4	105.2 ± 1.9	148.4 ± 2.6	36.0 ± 0.5	9.7 ± 0.1
Sum of ethyl methyl naphthalene	EMNAPH	580.5 ± 25.0	901.1 ± 44.3	259.9 ± 23.4	393.0 ± 22.7	29.9 ± 1.1	15.4 ± 1.1	24.0 ± 1.0	43.0 ± 1.5	15.9 ± 0.5	6.9 ± 0.3
Acenaphthylene	ACNAPY	320.6 ± 23.2	484.5 ± 43.5	156.6 ± 16.2	232.4 ± 30.5	342.7 ± 14.2	48.9 ± 2.9	190.8 ± 8.3	215.5 ± 9.7	62.9 ± 2.0	15.1 ± 0.5
Acenaphthene	ACNAPE	95.3 ± 31.2	190.5 ± 61.4	0.1 ± 11.4	136.1 ± 20.6	38.8 ± 6.0	1.1 ± 0.3	27.0 ± 3.8	5.3 ± 1.0	4.1 ± 0.4	0.0 ± 0.1
Fluorene	FLUORE	440.4 ± 16.6	532.5 ± 27.2	348.3 ± 18.9	238.9 ± 12.2	65.2 ± 2.5	15.0 ± 0.7	60.1 ± 2.7	100.7 ± 4.6	17.7 ± 0.5	6.7 ± 0.2
Phenanthrene	PHENAN	706.2 ± 21.1	1054.3 ± 40.0	358.1 ± 13.7	283.1 ± 10.3	94.2 ± 2.5	31.8 ± 1.0	87.9 ± 3.4	158.1 ± 4.8	36.9 ± 0.8	18.3 ± 0.4
Sum of methyl flourenes	MFLUOR	198.8 ± 16.6	273.7 ± 30.4	123.8 ± 13.6	253.7 ± 15.8	19.9 ± 0.9	5.5 ± 0.4	14.9 ± 0.8	32.5 ± 1.8	6.0 ± 0.3	1.5 ± 0.1
9-fluorenone	FL9ONE	2790.3 ± 85.7	4002.3 ± 159.3	1578.4 ± 63.2	961.0 ± 38.3	39.3 ± 1.1	25.1 ± 0.8	51.7 ± 2.0	119.1 ± 3.7	33.8 ± 0.8	22.5 ± 0.6
Xanthone	XANONE	35.0 ± 3.5	57.2 ± 6.5	12.8 ± 2.6	13.6 ± 4.5	2.9 ± 0.2	3.1 ± 0.2	3.6 ± 0.3	13.0 ± 0.7	2.3 ± 0.1	2.2 ± 0.1
Acenaphthenequinone	ACQUONE	29.9 ± 3.2	59.7 ± 6.1	0.0 ± 2.0	0.0 ± 4.2	0.3 ± 0.0	0.6 ± 0.1	0.5 ± 0.1	0.7 ± 0.1	0.0 ± 0.0	0.0 ± 0.0
Perinaphthenone	PNAPONE	532.9 ± 31.5	762.7 ± 58.8	303.1 ± 22.6	223.6 ± 18.7	2.0 ± 0.1	3.9 ± 0.3	5.2 ± 0.3	22.1 ± 1.2	2.8 ± 0.1	2.6 ± 0.1
Sum of methyl phenanthrene	MPHEN	291.5 ± 17.3	448.4 ± 30.7	134.7 ± 16.1	91.4 ± 10.7	17.4 ± 0.5	16.3 ± 0.7	22.4 ± 0.8	74.2 ± 2.0	12.4 ± 0.3	6.9 ± 0.2
Sum of di-methyl phenanthrene	DMPHEN	142.2 ± 10.0	244.3 ± 18.6	40.1 ± 7.2	93.5 ± 11.6	5.5 ± 0.2	66.3 ± 3.1	7.7 ± 0.3	36.9 ± 1.0	4.7 ± 0.1	3.5 ± 0.1
Anthracene	ANTHRA	36.0 ± 8.1	60.2 ± 14.7	11.7 ± 6.6	25.5 ± 5.2	18.2 ± 1.2	6.3 ± 0.5	19.4 ± 1.8	39.5 ± 3.1	7.5 ± 0.4	3.4 ± 0.2
Fluoranthene	FLUORA	1253.4 ± 46.1	1826.0 ± 86.2	680.9 ± 32.5	326.0 ± 17.5	12.5 ± 0.4	10.5 ± 0.4	28.1 ± 1.5	73.8 ± 3.1	9.1 ± 0.3	7.7 ± 0.2
Pyrene	PYRENE	1404.2 ± 49.5	2083.3 ± 93.1	725.2 ± 33.4	516.8 ± 25.6	11.7 ± 0.4	16.1 ± 0.8	30.1 ± 1.5	80.2 ± 3.1	11.1 ± 0.4	9.0 ± 0.3
Retene	RETENE	3.1 ± 5.2	6.1 ± 9.7	0.0 ± 3.6	0.0 ± 6.0	0.0 ± 0.1	1.3 ± 0.2	0.0 ± 0.1	0.1 ± 0.1	0.2 ± 0.0	0.1 ± 0.0
Sum of methylpyrenes	MFLPYR	264.1 ± 38.4	429.0 ± 65.7	99.1 ± 39.6	185.2 ± 38.5	2.0 ± 3.5	28.2 ± 11.3	4.7 ± 4.3	10.6 ± 6.1	1.3 ± 2.3	1.2 ± 1.7
Benzo(c)phenanthrene	BZCPHEN	0.2 ± 4.3	0.2 ± 7.8	0.3 ± 3.6	0.0 ± 6.3	0.2 ± 0.1	0.1 ± 0.1	0.4 ± 0.1	0.4 ± 0.1	0.1 ± 0.0	0.0 ± 0.0
Benz(a)anthracene	BAANTH	151.6 ± 11.2	302.7 ± 21.3	0.4 ± 7.0	140.0 ± 14.0	0.9 ± 0.1	0.6 ± 0.1	0.3 ± 0.1	1.3 ± 0.2	0.5 ± 0.0	0.3 ± 0.0
Chrysene	CHRYSN	132.1 ± 13.4	207.9 ± 25.0	56.3 ± 9.9	78.9 ± 11.4	0.9 ± 0.1	0.7 ± 0.1	0.6 ± 0.1	0.7 ± 0.1	0.2 ± 0.0	0.1 ± 0.0
Benzo(b+j+k)fluoranthene	BBJKFL	28.2 ± 6.1	56.3 ± 11.8	0.1 ± 3.2	0.0 ± 6.8	4.7 ± 0.5	2.3 ± 0.3	4.2 ± 0.4	2.3 ± 0.3	1.7 ± 0.1	0.6 ± 0.1
BeP	BEPYRN	2.0 ± 2.7	2.2 ± 4.9	1.8 ± 2.2	0.0 ± 4.2	2.8 ± 0.3	1.2 ± 0.1	3.4 ± 0.3	1.7 ± 0.2	1.3 ± 0.1	0.5 ± 0.0
BaP	BAPYRN	4.8 ± 8.5	7.2 ± 15.6	2.4 ± 6.7	2.4 ± 13.6	3.3 ± 0.5	1.3 ± 0.3	3.1 ± 0.4	1.4 ± 0.3	0.8 ± 0.1	0.2 ± 0.1
Indeno[123-cd]pyrene	INCDPY	0.1 ± 7.1	0.2 ± 13.1	0.0 ± 5.4	0.0 ± 11.4	4.0 ± 0.5	2.1 ± 0.4	3.8 ± 0.5	1.3 ± 0.3	3.2 ± 0.3	1.5 ± 0.1
Benzo(ghi)perylene	BGHIPE	0.0 ± 9.2	0.0 ± 17.0	0.0 ± 7.0	0.3 ± 14.8	10.5 ± 1.2	7.5 ± 1.2	10.9 ± 1.3	3.0 ± 0.5	8.5 ± 0.8	3.8 ± 0.3
Dibenzo(ah+ac)anthracene	DBANTH	0.0 ± 10.2	0.0 ± 18.9	0.0 ± 7.8	0.0 ± 16.5	0.1 ± 0.1	0.1 ± 0.1	0.1 ± 0.2	0.0 ± 0.2	0.1 ± 0.1	0.0 ± 0.0
Coronene	CORONE	0.0 ± 2.6	0.0 ± 4.9	0.0 ± 2.0	0.0 ± 4.2	8.8 ± 1.3	7.2 ± 1.7	11.1 ± 1.9	2.8 ± 0.5	6.4 ± 0.7	3.2 ± 0.4
<u>Alkanes (ug/mile)</u>											
Norfarnesane	NORFARN	118.2 ± 10.2	141.8 ± 16.4	94.6 ± 12.3	362.1 ± 29.5	1.7 ± 0.3	0.0 ± 0.1	7.5 ± 0.6	18.1 ± 1.4	0.0 ± 0.0	0.0 ± 0.0
Farnesane	FARNES	33.2 ± 14.1	34.2 ± 23.6	32.1 ± 15.5	640.1 ± 74.0	2.4 ± 0.6	0.1 ± 0.3	1.4 ± 0.3	16.6 ± 2.0	0.0 ± 0.0	0.0 ± 0.0
Norpristane	NORPRIS	491.9 ± 35.2	548.2 ± 54.9	435.6 ± 44.1	841.8 ± 75.3	1.0 ± 0.4	0.0 ± 0.2	0.9 ± 0.2	19.9 ± 2.0	0.0 ± 0.0	0.0 ± 0.0
Pristane	PRIST	179.1 ± 18.0	358.2 ± 36.0	0.0 ± 2.0	30.4 ± 7.1	1.7 ± 0.3	0.5 ± 0.1	0.5 ± 0.1	0.3 ± 0.1	0.0 ± 0.0	0.0 ± 0.0
Phytane	PHYTAN	306.3 ± 47.4	406.8 ± 85.4	205.7 ± 41.3	703.9 ± 64.9	1.1 ± 0.5	0.0 ± 0.3	0.7 ± 0.3	8.1 ± 1.2	0.0 ± 0.0	0.0 ± 0.0
Sum of cyclohexanes	NCYHEXS	3808.7 ± 235.7	4458.7 ± 212.2	3158.7 ± 421.2	2538.7 ± 331.3	11.5 ± 3.9	39.5 ± 3.9	14.4 ± 2.1	64.1 ± 3.1	0.0 ± 0.0	0.0 ± 0.0
<u>Polar Compounds (ug/mile)</u>											
tridecanoic acid (c13)	TDECAC	8.1 ± 14.6	12.0 ± 27.7	4.1 ± 9.0	0.0 ± 7.3	0.3 ± 0.1	0.3 ± 0.1	0.3 ± 0.1	2.5 ± 0.4	0.1 ± 0.1	0.1 ± 0.1
phthalic acid	PHTHAC	1357.3 ± 175.8	2658.5 ± 350.1	56.1 ± 33.2	381.1 ± 94.8	0.0 ± 1.0	0.0 ± 0.5	1.2 ± 0.6	11.5 ± 3.8	0.0 ± 0.5	0.2 ± 0.6
glutaric acid (d-c5)	GLUAC	170.9 ± 43.7	339.2 ± 87.0	2.6 ± 7.5	27.4 ± 17.2	0.0 ± 0.2	0.0 ± 0.1	0.0 ± 0.2	1.5 ± 0.6	0.0 ± 0.2	0.0 ± 0.2
succinic acid (d-c4)	SUCAC	192.4 ± 73.7	372.6 ± 146.3	12.2 ± 18.0	270.6 ± 65.0	0.0 ± 0.5	0.0 ± 0.4	0.0 ± 0.2	0.0 ± 1.4	0.0 ± 0.3	0.0 ± 0.5

Table S3 (continued). Speciated emission rates for composite diesel and gasoline exhaust profiles.

Species Description	Nmemonic	HDD	HCS	HW	MDD	SI_BC	SI_BW	SI_HC	SI_HW	SI_LC	SI_LW
<u>Steranes (ug/mile)</u>											
C27-20S-13 β (H),17a(H)-diasterane	STER35	44.8 \pm 3.3	59.5 \pm 6.1	30.1 \pm 2.7	34.1 \pm 11.2	0.4 \pm 0.1	0.3 \pm 0.1	1.7 \pm 0.2	1.3 \pm 0.1	0.3 \pm 0.0	0.3 \pm 0.0
C27-20R-13 β (H),17a(H)-diasterane	STER36	28.6 \pm 3.1	33.2 \pm 5.4	24.1 \pm 2.9	25.3 \pm 11.2	0.2 \pm 0.0	0.2 \pm 0.0	1.3 \pm 0.1	1.0 \pm 0.1	0.1 \pm 0.0	0.1 \pm 0.0
C28-20S-13 β (H),17a(H)-diasterane	STER39	7.5 \pm 2.8	0.3 \pm 4.9	14.7 \pm 2.8	23.2 \pm 12.0	0.2 \pm 0.0	0.1 \pm 0.1	1.3 \pm 0.2	0.9 \pm 0.1	0.1 \pm 0.0	0.1 \pm 0.0
C27-20S5a(H),14a(H)-cholestane	STER42	25.8 \pm 3.5	31.6 \pm 6.4	20.0 \pm 3.1	16.2 \pm 11.2	0.1 \pm 0.0	0.2 \pm 0.1	1.1 \pm 0.2	0.0 \pm 0.0	0.1 \pm 0.0	0.1 \pm 0.0
C27-20R5a(H),14 β (H)-cholestane	STER43	29.8 \pm 4.5	43.1 \pm 8.4	16.5 \pm 3.3	24.1 \pm 12.1	0.5 \pm 0.1	0.3 \pm 0.1	3.9 \pm 0.6	2.6 \pm 0.3	0.5 \pm 0.1	0.3 \pm 0.0
C27-20S5a(H),14 β (H),17 β (H)-cholestane	STER44	33.6 \pm 4.9	0.6 \pm 4.9	66.5 \pm 8.4	15.3 \pm 11.3	0.4 \pm 0.1	0.2 \pm 0.1	1.9 \pm 0.3	1.6 \pm 0.2	0.2 \pm 0.0	0.2 \pm 0.0
C27-20R5a(H),14a(H),17a(H)-cholestane&C29-20S13 β (H),17a(H)-diasterane	STER45_40	14.7 \pm 3.1	0.8 \pm 4.9	28.7 \pm 3.9	41.9 \pm 12.2	0.5 \pm 0.1	0.4 \pm 0.1	5.0 \pm 0.7	4.2 \pm 0.5	0.6 \pm 0.1	0.8 \pm 0.1
C28-20R5a(H),14 β (H),17 β (H)-ergostane	STER47	0.6 \pm 2.6	0.9 \pm 4.9	0.2 \pm 2.0	22.8 \pm 12.0	0.1 \pm 0.0	0.1 \pm 0.1	1.2 \pm 0.2	1.2 \pm 0.2	0.2 \pm 0.0	0.8 \pm 0.1
C28-20S5a(H),14 β (H),17 β (H)-ergostane	STER48	0.0 \pm 2.6	0.0 \pm 4.9	0.0 \pm 2.0	0.0 \pm 11.2	0.2 \pm 0.0	0.1 \pm 0.0	1.7 \pm 0.2	0.9 \pm 0.1	0.0 \pm 0.0	0.1 \pm 0.0
C28-20R5a(H),14a(H),17a(H)-ergostane	STER49	0.2 \pm 2.6	0.2 \pm 4.9	0.2 \pm 2.0	24.4 \pm 11.6	0.7 \pm 0.1	0.7 \pm 0.1	1.9 \pm 0.3	3.8 \pm 0.5	1.6 \pm 0.1	3.7 \pm 0.3
C29-20S5a(H),14a(H),17a(H)-stigmastane	STER50	0.1 \pm 2.6	0.2 \pm 4.9	0.1 \pm 2.0	8.5 \pm 11.2	0.2 \pm 0.0	0.1 \pm 0.0	1.4 \pm 0.2	0.8 \pm 0.1	0.1 \pm 0.0	0.0 \pm 0.0
C29-20R5a(H),14 β (H),17 β (H)-stigmastane	STER51	0.3 \pm 2.6	0.4 \pm 4.9	0.2 \pm 2.0	14.0 \pm 11.2	0.3 \pm 0.1	0.1 \pm 0.1	3.2 \pm 0.5	2.0 \pm 0.4	0.1 \pm 0.0	0.0 \pm 0.0
C29-20S5a(H),14 β (H),17 β (H)-stigmastane	STER52	0.4 \pm 2.6	0.5 \pm 4.9	0.3 \pm 2.0	0.0 \pm 11.2	0.2 \pm 0.0	0.4 \pm 0.0	3.4 \pm 0.2	3.4 \pm 0.2	0.5 \pm 0.0	0.1 \pm 0.0
C29-20R5a(H),14a(H),17a(H)-stigmastane	STER53	0.2 \pm 2.6	0.2 \pm 4.9	0.1 \pm 2.0	1.4 \pm 11.2	0.3 \pm 0.1	0.2 \pm 0.1	2.0 \pm 0.3	1.2 \pm 0.2	0.2 \pm 0.0	0.0 \pm 0.0
<u>Hopananes (ug/mile)</u>											
18a(H),21 β (H)-22,29,30-Trisnorhopane	HOP13	41.7 \pm 4.6	82.9 \pm 9.1	0.5 \pm 2.0	6.2 \pm 11.3	0.0 \pm 0.1	0.7 \pm 0.2	1.9 \pm 0.3	0.8 \pm 0.2	0.0 \pm 0.0	0.0 \pm 0.0
17a(H),21 β (H)-22,29,30-Trisnorhopane	HOP15	0.1 \pm 2.6	0.0 \pm 4.9	0.1 \pm 2.0	0.0 \pm 11.2	0.3 \pm 0.3	0.4 \pm 0.3	1.4 \pm 0.9	2.4 \pm 1.3	0.1 \pm 0.1	0.1 \pm 0.1
17a(H),21 β (H)-30-Norhopane	HOP17	124.1 \pm 17.2	193.4 \pm 33.0	54.7 \pm 9.5	34.6 \pm 17.6	0.7 \pm 0.2	0.5 \pm 0.1	10.9 \pm 1.0	6.6 \pm 0.9	0.2 \pm 0.1	0.1 \pm 0.0
17a(H),21 β (H)-Hopane	HOP19	56.4 \pm 6.5	89.5 \pm 12.4	23.3 \pm 3.7	82.4 \pm 12.4	4.6 \pm 0.9	3.8 \pm 0.7	16.5 \pm 2.0	16.1 \pm 1.7	0.0 \pm 0.0	0.0 \pm 0.0
22S-17a(H),21 β (H)-30-Homohopane	HOP21	0.2 \pm 2.6	0.0 \pm 4.9	0.4 \pm 2.0	4.5 \pm 11.2	0.0 \pm 0.1	0.0 \pm 0.1	3.9 \pm 0.4	2.2 \pm 0.4	0.1 \pm 0.0	0.0 \pm 0.0
22R-17a(H),21 β (H)-30-Homohopane	HOP22	0.0 \pm 2.6	0.0 \pm 4.9	0.1 \pm 2.0	6.9 \pm 11.3	2.9 \pm 0.7	1.9 \pm 0.5	9.2 \pm 1.4	5.3 \pm 1.1	0.0 \pm 0.0	0.0 \pm 0.0
22S-17a(H),21 β (H)-30,31-Bishomohopane	HOP24	0.0 \pm 2.6	0.0 \pm 4.9	0.0 \pm 2.0	1.4 \pm 11.2	0.0 \pm 0.0	0.1 \pm 0.0	1.8 \pm 0.2	1.2 \pm 0.1	0.1 \pm 0.0	0.0 \pm 0.0
22R-17a(H),21 β (H)-30,31-Bishomohopane	HOP25	0.0 \pm 2.6	0.0 \pm 4.9	0.0 \pm 2.0	0.0 \pm 11.2	0.0 \pm 0.0	0.0 \pm 0.0	1.3 \pm 0.2	0.8 \pm 0.2	0.1 \pm 0.0	0.0 \pm 0.0
22S-17a(H),21 β (H)-30,31,32-Trisomohopane	HOP26	0.0 \pm 2.6	0.0 \pm 4.9	0.0 \pm 2.0	0.0 \pm 11.2	0.1 \pm 0.1	0.1 \pm 0.1	1.7 \pm 0.3	0.8 \pm 0.3	0.1 \pm 0.0	0.0 \pm 0.0

Data Quality and Analysis of Dilution Tunnel Blanks

Figure S1 shows comparisons of PM emission rates determined by BKI and UWV from their primary dilution tunnels versus the corresponding gravimetric mass data obtained by DRI from the secondary dilution tunnel sampler. The generally good agreement between PM mass measured prior to and after the secondary dilution sampler indicates that the additional residence time and secondary dilution, in the case of the CI tests, had little effect on the measured gravimetric mass. Reconstruction of the total mass concentration by summing the TOR, IC, AC, and XRF species gives good agreement with gravimetric mass as shown in Figure S2. As expected, the reconstructed mass is slightly less since elements have not been converted to their common oxide forms and ammonium is the only cation included, and OC was not converted to organic matter by applying a factor (31) to account for the missing hydrogen, oxygen and other elements that may be present in organic compounds. Sulfate and potassium ions were subtracted from the XRF sulfur and potassium values. There is a positive offset in the material balance for diesel vehicles at lower concentrations, which is due to the semi-volatile carbon species that are emitted by diesel engines (e.g., fuel-related alkanes). These species are collected on the quartz filter and detected by TOR. They are not adsorbed by the Teflon filters that are weighed for mass concentration.

Table S3 shows the mass loadings in the dynamic blanks relative to composite SI and CI exhaust samples. Dynamic blanks were also composited for better analytical sensitivity. A total of six 58-minute blanks were collected during the light-duty vehicle phase, but one (blank #4) was invalidated due to a system malfunction. The first blank was collected prior to the initial vehicle test. Subsequent blanks were collected after vehicle category 2, and during category 5, 8, and 9. All blanks were collected prior to the start of the day's testing, except for the final blank (#6), which was collected about one hour after the last test of the day. The first three SI blanks are consistent in composition and were composited as SI_DB1. Blank 5 (SI_DB2) is similar to the first three but contains slightly increased amounts of higher temperature organic carbon and the elements Al, Ca, Si, and Fe. Ions, which are likely artifacts of ambient air infiltration, show similar proportions among the blanks. In contrast to the others, blank 6 (SI_DB3) contains substantial amounts of elemental carbon and higher concentrations of all organic carbon components plus relatively large concentrations of Zn, Ca, Fe, and Si. In addition, this sample

differs from the other dynamic blanks in that the gravimetric mass concentration is more consistent with the total carbon measured suggesting that the compounds evolved in the TOR analysis were primarily in the particle phase.

The speciation of heavy (5-7 rings) PAHs for the blanks is consistent with the exhaust samples, but the absolute concentrations measured were larger for the blanks than for many of the low-emitting vehicle tests. Thus, the dynamic blanks cannot be considered representative of 'background' levels for these compounds. Hopanes and steranes did not display any consistency in speciation for the dynamic blanks, due to the analytical uncertainty at such low concentrations. Finally, a very different composition of heavy PAH compounds is present in blank SI_DB3. All other dynamic blanks were collected at the start of the sampling day, whereas blank SI_DB3 was collected at the end of the day following vehicle tests with high emission levels that contaminated the exhaust dilution system.

A total of 11 blanks were collected during the CI phase and composited into 5 groups for analysis. These blanks were collected for 30 minutes, except the first and last blanks (blanks 9 and 3), which were run for 60 minutes. Although most dynamic blanks were collected prior to the start of the day's testing, several were also collected mid-day and one in the afternoon. The composition of the CI blanks was quite consistent except for Blank IIIIn, which was collected without secondary dilution. Blank 5 showed slightly increased amounts of the higher temperature carbon compounds, Ca, Si, and Fe, plus sulfate and Zn. Several samples have significant concentration of sulfate ion, which may be due, in large part, to ambient air infiltration. Total carbon measured on the quartz filters generally far exceeds the gravimetric mass on the Teflon filters similar to the SI blanks. The heavy PAHs in the blanks are not consistent in with the speciation in the exhaust compounds and hopanes and steranes concentrations in the blanks were not present in analytically significant levels.

Table S4. Mass loadings in dynamic blanks relative to composite SI and CI exhaust samples *.

Vehicle Group	Weight Class	Test Cycle	Secondary		PM2.5 mass (ug/m3)	Total Carbon (ug/m3)	OC (ug/m3)	EC (ug/m3)	particulate PAH (ng/m3)	Hopanes (ng/m3)	Steranes (ng/m3)
			Dilution Ratio								
SI_DB1	LD	Blank	1		2.2 +/- 2.7	14.9 +/- 1.6	14.1 +/- 1.6	0.8 +/- 0.3	383.6 +/- 34.4	5.3 +/- 7.7	58.0 +/- 3.7
SI_DB2	LD	Blank	1		6.1 +/- 2.7	24.2 +/- 1.8	21.4 +/- 1.8	2.8 +/- 0.3	540.3 +/- 99.7	8.6 +/- 18.7	107.3 +/- 24.7
SI_DB3	LD	Blank	1		107.8 +/- 2.8	113.3 +/- 4.3	51.1 +/- 3.0	62.2 +/- 2.6	263.9 +/- 49.8	1197.0 +/- 345.6	345.7 +/- 42.8
SI- 1	LD	UDC	1		169.3 +/- 1.1	108.3 +/- 2.9	77.4 +/- 3.2	31.0 +/- 0.9	873.3 +/- 110.5	18.3 +/- 6.0	53.1 +/- 4.9
SI- 2	LD	UDC	1		89.3 +/- 2.3	64.1 +/- 1.7	45.0 +/- 1.7	19.1 +/- 0.5	383.6 +/- 34.4	5.3 +/- 7.7	58.0 +/- 3.7
SI- 3	LD	UDC	1		33.3 +/- 1.1	27.5 +/- 1.0	19.4 +/- 0.9	8.2 +/- 0.3	25.8 +/- 6.1	13.1 +/- 7.5	111.7 +/- 11.4
SI- 4	LD	UDC	1		140.6 +/- 1.2	77.8 +/- 2.2	37.8 +/- 1.6	40.0 +/- 1.2	319.1 +/- 38.6	3.7 +/- 2.9	30.4 +/- 3.7
SI- 5	LD	UDC	1		112.1 +/- 1.6	91.5 +/- 1.3	67.8 +/- 1.4	23.7 +/- 0.4	93.4 +/- 8.1	1.4 +/- 1.5	165.0 +/- 6.2
SI- 6	LD	UDC	1		102.2 +/- 1.5	133.8 +/- 1.7	90.8 +/- 1.5	43.0 +/- 0.7	155.6 +/- 11.6	31.8 +/- 6.3	261.4 +/- 10.7
SI- 7	LD	UDC	1		346.2 +/- 1.8	331.9 +/- 4.6	280.0 +/- 6.2	51.9 +/- 0.7	171.1 +/- 10.7	670.5 +/- 54.0	493.8 +/- 18.0
SI- 8	LD	UDC	1		788.9 +/- 2.2	669.6 +/- 12.9	465.8 +/- 14.9	203.7 +/- 3.8	1618.9 +/- 137.4	975.6 +/- 70.5	525.5 +/- 22.1
SI- 9	LD	UDC	1		1055.2 +/- 1.7	962.4 +/- 13.5	307.5 +/- 5.7	654.9 +/- 11.8	6515.6 +/- 801.8	1640.2 +/- 105.6	476.2 +/- 24.9
SI-10	LD	UDC	1		2693.4 +/- 5.0	2428.2 +/- 31.4	1881.7 +/- 35.4	546.5 +/- 10.4	3828.9 +/- 228.5	2220.3 +/- 102.9	1958.5 +/- 64.2
Blank-3	Dyn	Blank	22		25.5 +/- 5.9	94.0 +/- 6.1	83.6 +/- 6.0	10.5 +/- 6.8	0.9 +/- 20.4		
Blank-9	Dyn	Blank	49		22.3 +/- 2.7	33.7 +/- 2.5	28.1 +/- 2.3	5.5 +/- 0.5	0.0 +/- 7.9		
Blank-I	Dyn	Blank	37		1.0 +/- 3.0	40.2 +/- 2.2	39.7 +/- 2.1	0.4 +/- 0.4	0.8 +/- 3.8		
Blank-III	Dyn	Blank	37		4.4 +/- 3.0	34.9 +/- 2.1	34.2 +/- 2.0	0.7 +/- 0.6	0.0 +/- 4.8		
HDD	I	HCS	40		40.8 +/- 2.2	85.2 +/- 2.1	55.4 +/- 1.7	29.9 +/- 0.7	2.4 +/- 4.1		
HDD	II	HCS	30		249.1 +/- 5.8	285.2 +/- 16.2	82.1 +/- 6.0	203.1 +/- 11.3	0.3 +/- 16.3	36.6 +/- 10.8	39.0 +/- 12.5
HDD	II	HCS	40		36.7 +/- 2.3	83.1 +/- 2.2	53.8 +/- 1.7	29.3 +/- 0.7	0.5 +/- 4.5	0.0 +/- 9.6	42.2 +/- 12.4
HDD	III	HCS	40		90.5 +/- 1.9	141.8 +/- 3.0	62.3 +/- 1.7	79.5 +/- 1.7	0.9 +/- 2.1	67.0 +/- 4.3	144.7 +/- 4.6
HDD	III	HCS	50		111.5 +/- 3.4	162.9 +/- 5.7	65.5 +/- 2.8	97.4 +/- 3.5	4.1 +/- 4.9	52.6 +/- 6.3	63.8 +/- 5.6
HDD	I	HW	40		43.4 +/- 2.3	97.2 +/- 2.5	61.0 +/- 1.9	36.2 +/- 0.8	1.2 +/- 2.9		
HDD	II	HW	30		556.5 +/- 6.3	621.7 +/- 34.8	166.8 +/- 11.0	454.9 +/- 25.3	0.0 +/- 17.1	41.3 +/- 13.2	72.6 +/- 13.9
HDD	II	HW	40		56.5 +/- 2.5	115.7 +/- 3.1	69.7 +/- 2.2	46.0 +/- 1.2	0.0 +/- 4.1		
HDD	III	HW	40		82.9 +/- 2.0	137.9 +/- 2.9	68.7 +/- 1.8	69.2 +/- 1.4	0.0 +/- 1.3	56.9 +/- 4.6	87.1 +/- 2.8
HDD	III	HW	50		114.6 +/- 3.0	168.5 +/- 5.3	66.3 +/- 2.6	102.2 +/- 3.4	0.0 +/- 4.9	46.6 +/- 5.7	121.4 +/- 6.4
Blank-IIIIn	Dyn	Blank	1		187.9 +/- 9.0	257.6 +/- 11.0	173.9 +/- 8.4	83.8 +/- 4.8	3.0 +/- 6.6		
HDD	III	HCS	1		4985.8 +/- 15.2	5063.4 +/- 206.4	1355.5 +/- 58.2	3707.9 +/- 155.2	89.9 +/- 18.9	46.3 +/- 9.5	137.7 +/- 9.6
HDD	III	HW	1		5799.9 +/- 13.2	4837.7 +/- 240.8	1763.9 +/- 98.1	3073.8 +/- 153.2	40.0 +/- 11.8	78.9 +/- 12.1	214.5 +/- 12.5

* Particulate PAH values are sum of benzo(b)fluoranthene, benzo(a)pyrene, benzo(ghi)perylene, indeno(1,2,3-cd)pyrene, dibenzo(ah+ac)anthracene and coronene, and carbon data are based on IMPROVE TOR method.

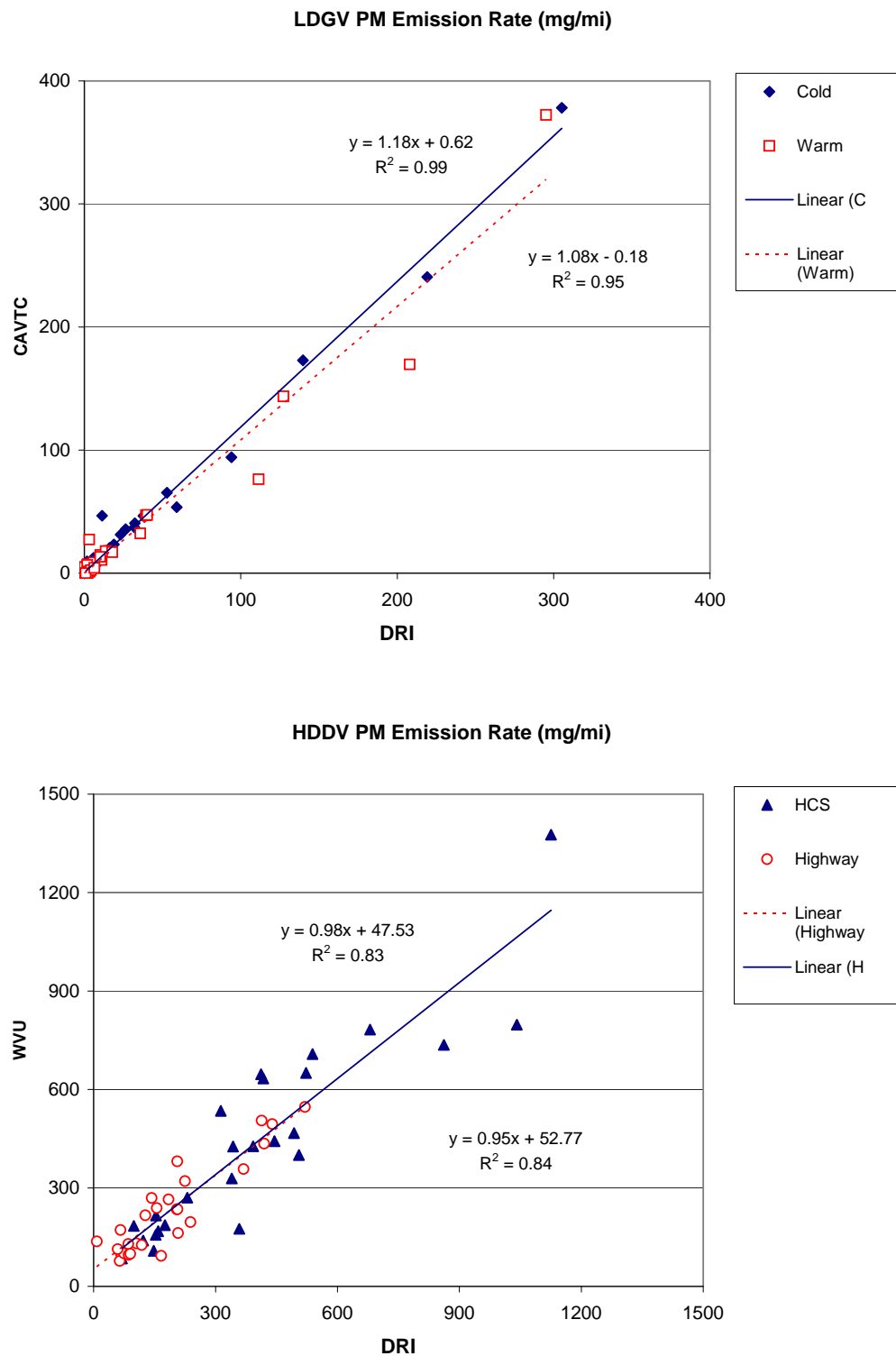


Figure S1. Comparisons of PM emission rates determined by EPA/BKI and UWV from their primary dilution tunnel versus the corresponding values obtained by DRI from the secondary dilution tunnel sampler.

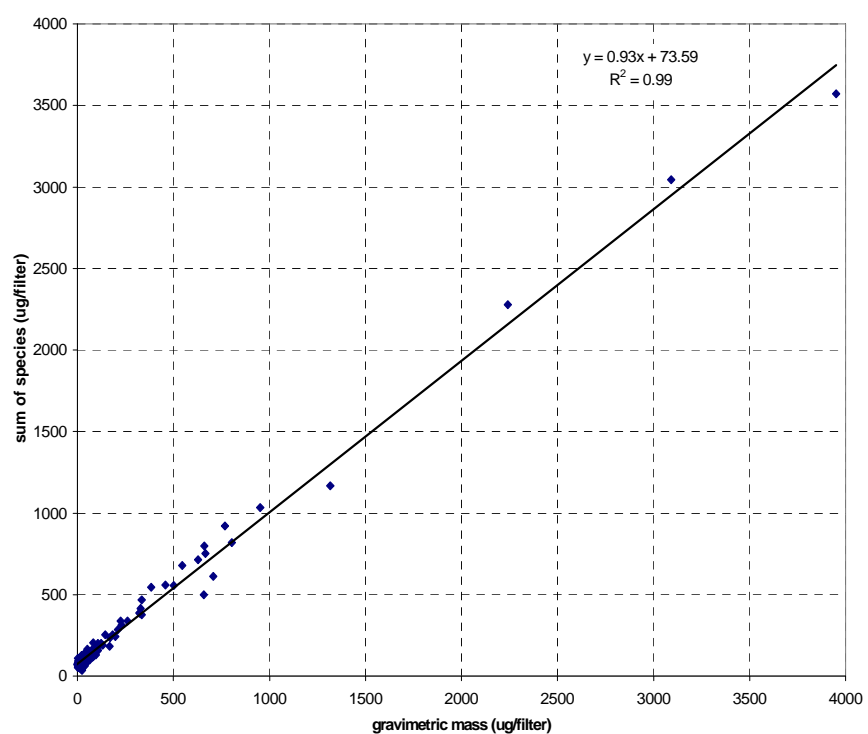
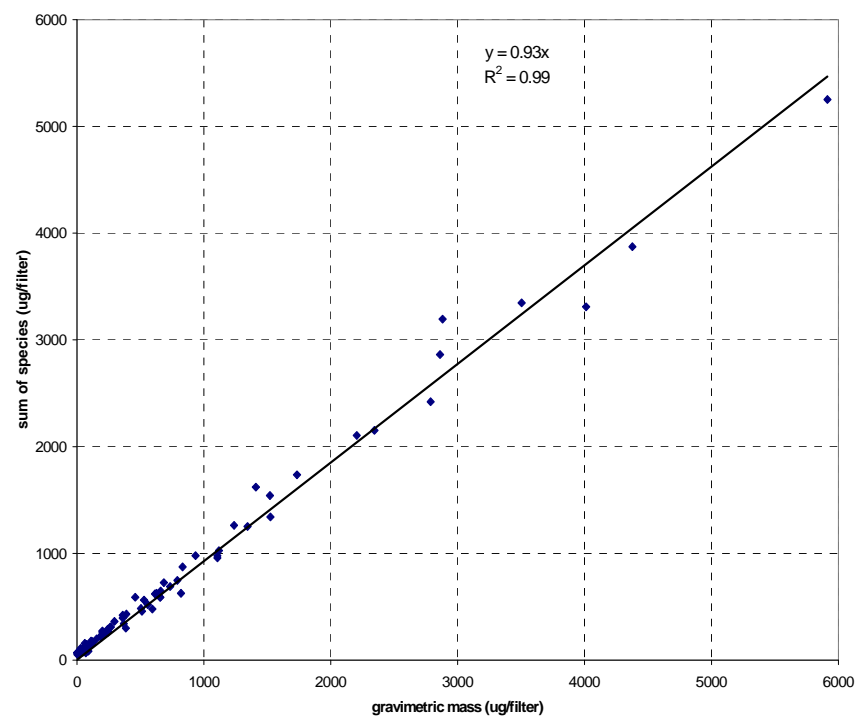


Figure S2. Correlation plot of gravimetric mass vs. sum of elements by XRF, ions by IC and AA, and carbon by TOR for light-duty vehicles (top panel) heavy-duty diesel vehicles (bottom panel).